Neubauer *et al. Swiss J Geosci* (2020) 113:21
https://doi.org/10.1186/s00015-020-00373-3

SGG SGS sc | nat
Swiss Journal of Geosciences

ORIGINAL PAPER Open Access

The Wechsel Gneiss Complex of Eastern Alps: an Ediacaran to Cambrian continental arc and its Early Proterozoic hinterland

Franz Neubauer[1*], Yongjiang Liu[2,3], Ruihong Chang[1], Sihua Yuan[1,4], Shengyao Yu[2,3], Johann Genser[1], Boran Liu[1] and Qingbin Guan[2,3]

Abstract

Many metamorphosed basement complexes in the Alps are polymetamorphic and their origin and geological history may only be deciphered by detailed geochronology on the different members including oceanic elements like ophiolites, arc successions, and continental passive margin successions. Here we present a case study on the Lower Austroalpine Variegated Wechsel Gneiss Complex and the overlying low-grade metamorphosed Wechsel Phyllite Unit at the eastern margin of Alps. The Wechsel Gneiss Complexes are known to have been overprinted by Devonian metamorphism, and both units were affected by Late Cretaceous greenschist facies metamorphism. New U–Pb zircon ages reveal evidence for two stages of continental arc-like magmatism at 500–520 Ma and 550–570 Ma in the Variegated Wechsel Gneiss Complex. An age of ca. 510 Ma of detrital zircons in metasedimentary rocks also constrain the maximum age of metasedimentary rocks, which is younger than Middle Cambrian. The overlying Wechsel Phyllite Unit is younger than 450 Ma (Late Ordovician) and seems to have formed by denudation of the underlying Variegated Wechsel Gneiss Complex. We speculate on potential relationships of the continental arc-type magmatism of the Variegated Wechsel Gneiss Complex and potential oceanic lithosphere (Speik complex) of Prototethyan affinity, which is also preserved in the Austroalpine nappe complex. The abundant, nearly uniform 2.1 Ga- and ca. 2.5 Ma-age signature of detrital zircons in metasediments (paragneiss, quartzite) of the Variegated Wechsel Gneiss Complex calls for Lower Proterozoic continental crust in the nearby source showing the close relationship to northern Gondwana prominent in West Africa and Amazonia.

Keywords: Subduction, Prototethys, Provenance, Neoproterozoic, Cambrian

1 Introduction

As known for a long time, the Austroalpine nappe complex of Eastern Alps and Western Carpathians contains two major basement units, which collided during the Variscan orogeny (e.g., Neubauer and Frisch 1993; Putiš et al. 2009; Vozárová et al. 2012, 2017). These include (1) a nearly unmetamorphic Gondwana-derived fossil-rich unit, which represents an Ordovician back-arc and a Devonian passive margin (Loeschke and Heinisch 1993; Schönlaub and Heinisch 1993; Neubauer and Sassi 1993); and (2) amphibolite-grade metamorphic units, which were fully affected by Variscan amphibolite-grade metamorphism including Devonian, early Variscan high-pressure metamorphism (Thöni 1999, 2006; Neubauer et al. 1999) (Fig. 1a). Some of these units are considered to represent, in major portions, a poorly dated magmatic arc system with intermediary and acidic orthogneisses (Schulz et al. 2004, 2008; Siegesmund et al. 2007, 2018; Mandl et al. 2018). Among these, the Lower Austroalpine Monotonous and Variegated Wechsel Gneiss Complexes of the Wechsel window shows Devonian pressure-dominated metamorphism in upper greenschist metamorphic

Editorial handling: Othmar Müntener

*Correspondence: franz.neubauer@sbg.ac.at
[1] Department of Geography and Geology, Geology Division, Paris-Lodron-University of Salzburg, Hellbrunnerstraße 34, 5020 Salzburg, Austria
Full list of author information is available at the end of the article

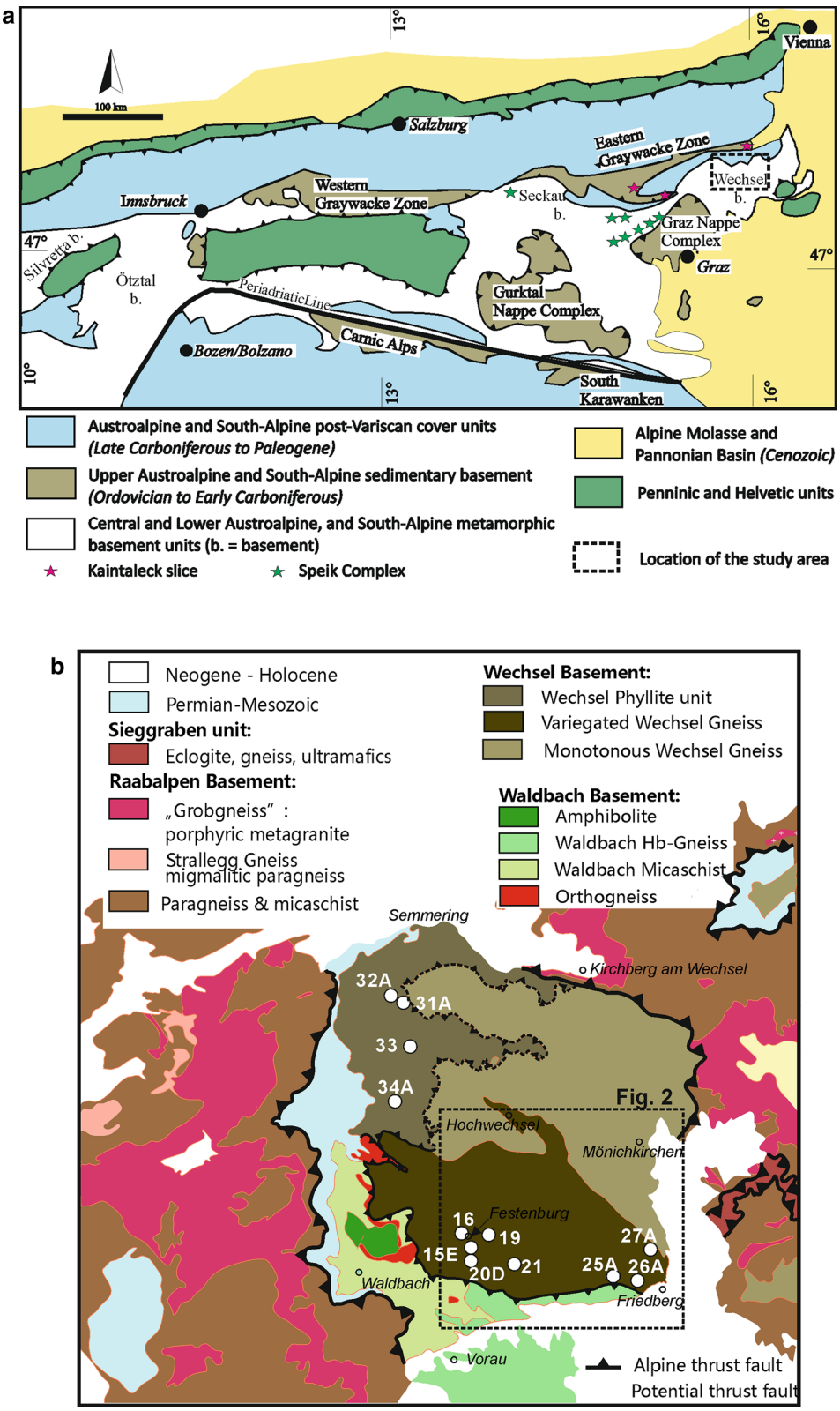

Fig. 1 **a** Location of the Wechsel window within the Eastern Alps. **b** Lower Austroalpine units at the eastern termination of Eastern Alps

conditions (Müller et al. 1999). On the other hand, several amphibolite-grade metamorphosed ophiolite successions were reported from the Austroalpine basement, too (Neubauer et al. 1989). The temporal relationship between potential arc successions and ophiolites is poorly known, mostly because missing protolith ages make any correlation between ophiolites and arc successions speculative.

In this contribution, we report the first protolith ages and geochemical constraints for both the Variegated Wechsel Gneiss Complex and the Wechsel Phyllite Unit and demonstrate two stages of Late Ediacaran and Cambrian arc magmatism. Based on detrital zircon ages of accompanying country rocks including feldspar-rich porphyroblastic albite-paragneisses we also show distinct Neoproterozoic to Cambrian age populations and a prominent nearby Early Proterozoic continental source. We finally discuss the paleogeographic and tectonic implications of these findings.

2 Regional geological setting

The Wechsel window exposes the deepest Austroalpine structural unit and contains two different pre-Alpine basement complexes, the Wechsel Gneiss Complex with the overlying Wechsel Phyllite Unit along its northwestern margin and the Waldbach-Vorau Complex (Faupl 1970a; Vetters 1970; Herrmann et al. 1991; Kreuss 2015; Fig. 1b). Both units are covered by a low-grade metamorphosed Permian to Upper Triassic siliciclastic-dolomitic cover strata (Angeiras 1967; Faupl 1970a, b; Vetters 1970; Tollmann 1977), which separates the Wechsel window from the overlying Kirchberg-Stuhleck nappe with its entirely different orthogneiss-rich basement dominated by Upper Paleozoic porphyric granite gneisses, the "Grobgneis" (Yuan et al. 2020). Along its western part, a small slice of Permian siliciclastic rocks also separates the Wechsel Gneiss Complex from the Waldbach-Vorau Complex (Huska 1970; Vetters 1970).

The geology of the study area is shown in two detailed geological maps (Herrmann et al. 1991; Kreuss 2015). The Wechsel basement within the Wechsel window comprises three units from base to top (Figs. 1b, 2, 3): (1) the Monotonous Wechsel Gneiss unit, (2) the Variegated Wechsel Gneiss unit, and (3) the Wechsel Phyllite Unit ("Wechselschiefer" of Faupl 1970a; Neubauer and Frisch 1993). In the field, albite porphyroblasts with sizes of 3–8 mm (Fig. 4) represent the most pronounced feature of both Monotonous and Variegated Wechsel Gneiss units (Richarz 1911; Mohr 1912, 1913; Schwinner 1932; Faupl 1970a, b; Huska 1971; Neubauer 1983; Neubauer and Frisch 1993), and the distinction between Monotonous and Variegated Wechsel Gneiss Complex was mapped and proposed by Neubauer (1983), (1994). The rocks have been described by several studies including Angeiras (1967), Faupl (1970a, b) and Vetters (1970). Both Montonous and Variegated Wechsel Gneiss Complexes include the ubiquitous albite porphyroblasts with a volume percentage of 20 to 40 percent in paragneiss and mafic rocks, the presence of chlorite in paragneiss and chlorite ± epidote and amphibole in mafic rocks, and the nearly complete obliteration of any primary feature. The Monotonous Wechsel Gneiss Complex includes mainly paragneiss and only few greenschist lenses (Fig. 2), whereas garnet-micaschist, orthogneiss, many mafic lenses, a single folded layer of a white quartzite, often slightly dark-coloured paragneisses and black micaschist and black quartzite characterize the overlying Variegated Wechsel Gneiss Complex (Figs. 2, 3). The boundary of both complexes are folded in map-scale overturned folds (Fig. 2).

The nature of the boundary between the Wechsel Gneiss Complexes and the Wechsel Phyllite Unit, tectonic or primary, remains unclear because of poor exposure (Faupl 1970a). In the northwestern Wechsel window, there is solely a difference in the content of porphyroblastic albite and a large difference in grain size between these two units. Further south, there is a significant difference between the higher-grade epidote–amphibolite to higher greenschist facies metamorphism with coarse albite porphyroblasts of the Variegated Wechsel Gneiss Complex and the Wechsel Phyllite Unit with its fine-grained phyllitic rocks metamorphosed within lower greenschist facies conditions. Within the northwestern Wechsel, Faupl (1970a) distinguished a ca. 180 m thick Lower Wechsel Phyllite Fm. from the Upper Wechsel Phyllite Fm (Fig. 3). The Lower Wechsel Phyllite Fm. contains mostly fine-grained feldspar- and chlorite-rich metatuffaceous rocks, the Upper Wechsel Phyllite Fm. black phyllites and quartz-phyllites with less volcanic input (Faupl 1970a).

In the Variegated and Monotonous Wechsel Gneiss Complexes exposed along the eastern edge of the Wechsel window, Müller et al. (1999) found evidence for Devonian (ca. 375 Ma) pressure dominated metamorphism, based on the high phengite content of white mica and Rb–Sr and Ar–Ar ages of coarse-grained white mica (150–300 µm). Further Ar–Ar and Rb–Sr ages of fine-grained white mica (100–125 µm) peculiarly in shear zones overprinting the earlier coarse-grained fabric in the eastern Wechsel window, two stages of low-grade (< 350 °C) metamorphic overprints (270–240 Ma and 70–80 Ma) were found (Müller et al. 1999). The dates of 270–240 Ma remain unclear and overlap in time with the age of the Permian to Lower Triassic cover succession. The Late Cretaceous metamorphic stage (70–80 Ma) affected the Permian to Triassic cover succession, too,

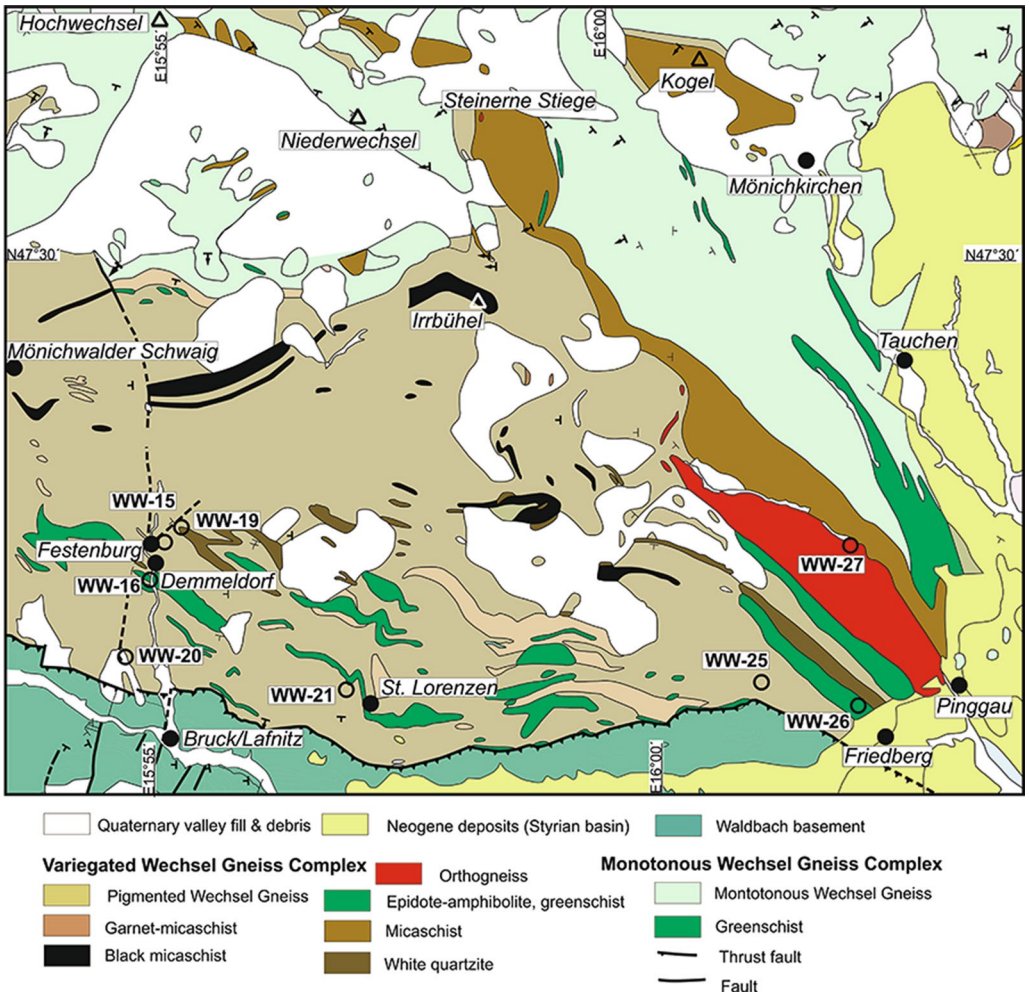

Fig. 2 Geological map of the southern Wechsel window and sample locations (mapped by Neubauer (1983), after compilation of Kreuss (2015))

and is directly related to Early Alpidic nappe stacking associated with ductile shearing of the deep structural level contemporaneous with sedimentation in Late Cretaceous Gosau basins at top of the Upper Austroalpine units within the Austroalpine nappe complex (Neubauer 1994).

To the south, the Variegated Wechsel Gneiss Complex is structurally delimited by a ductile shear zone of supposed Cretaceous age from the overlying Waldbach-Vorau Complex, which contains entirely different retrogressed amphibolite-grade mafic and felsic rocks (gabbro, metadiorite, hornblende-gneiss, augengneiss, orthogneiss) of entirely unknown protolith ages (Faupl 1970b; Huska 1970; Neubauer and Frisch 1993). The main stage of amphibolite facies-grade metamorphism of the Waldbach-Vorau Complex is believed to be Variscan, the retrogressive overprint in greenschist facies is Early Alpine (Late Cretaceous; Dallmeyer et al. 1996; Hoinkes et al. 1999).

3 Material and petrographic description

For U–Pb zircon dating, many samples of greenschists, an orthogneiss sample and several samples of metasedimentary rocks were collected from the Variegated Wechsel Gneiss Complex and low-grade rocks from the Wechsel Phyllite Unit (Table 1; for locations, see Figs. 1b, 2). We selected samples from the Variegated Wechsel Gneiss Complex because of its high variety of lithologies including mafic rocks and an orthogneiss body. The Monotonous Wechsel Gneiss Complex is exposed in the structural footwall of the Variegated Wechsel Gneiss Complex and includes only some greenschist lenses close to its northern margin (Fig. 2). Only one sample of a mafic rock of the Variegated Wechsel Gneiss Complex yielded sufficient zircons for dating (WW-26A, epidote–amphibolite).

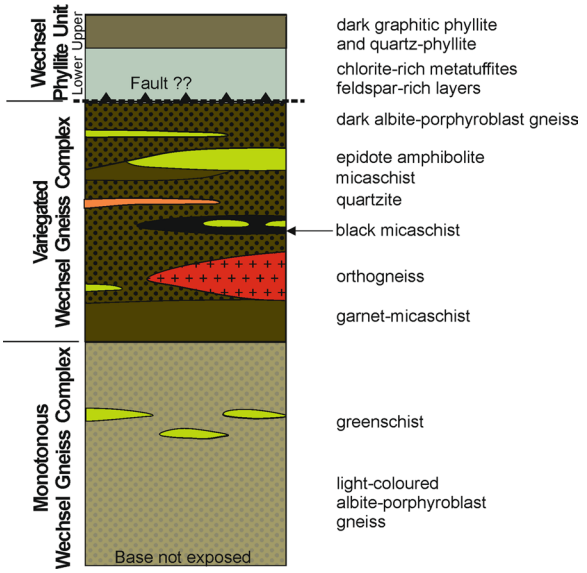

Fig. 3 Lithostratigraphic section of the Wechsel basement (modified from Neubauer et al. (1992))

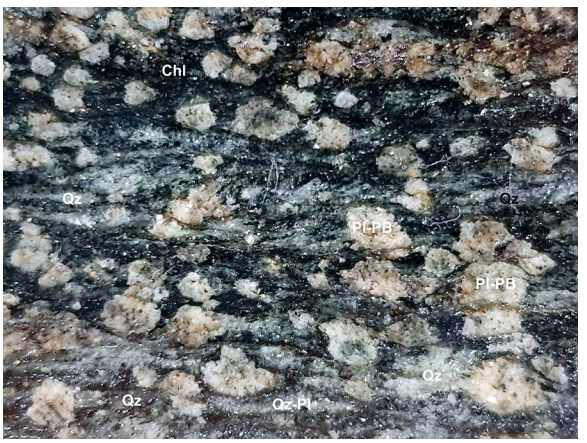

Fig. 4 Representative photographs of a typical porphyroblast-bearing Wechsel Gneiss. The rock is cut parallel to the stretching lineation and perpendicular to the foliation. The short axis of the image is ca. 4 cm. Chl: chlorite, Pl: plagioclase, Qz: quartz, Pl-PB: albite porphyroblast

Furthermore, a leucocratic orthogneiss (WW-27) and four metasedimentary rocks, including various types of albite-paragneisses (WW-16, WW-21, WW-25), and a quartzite sample (WW-19A) from the Variegated Wechsel Gneiss unit were suited for U–Pb dating, as were three plagioclase-rich, metatuffaceous samples from the Lower (samples WW-31A, WW-32A, WW-34A) and one of the Upper Wechsel Phyllite Fms. (WW-33A).

In the following, the typical rock types are described, particularly the ones used for U–Pb zircon dating and for geochemical analysis. Sample locations and mineralogy are summarized in Table 1 and representative photomicrographs are shown in Additional file 1: Figure S1 and Additional file 2: Figure S2.

3.1 Variegated Wechsel Gneiss Complex

Epidote–amphibolite and greenschist with albite porphyroblasts (Additional file 1: Figure S1b): The mineral assemblage contains albite, chlorite, amphibole, epidote, quartz, garnet, and opaque ores. These rocks always contain variable amounts of ovoid-shaped albite porphyroblasts and are characterized by the assemblage amphibole and chlorite. The foliation is often well developed. Amphibole has nearly no inclusions in contrast to the inclusion-rich albite porphyroblasts.

Epidote–amphibolite without albite porphyroblasts (Additional file 1: Figure S1h): Amphibole, clinozoisite, garnet, chlorite, albite, quartz, ilmenite and titanite are the main and minor minerals. These minerals form a massive fabric with clinozoisite and garnet porphyroblasts bearing many inclusions. Garnet (up to 3 mm in size) includes a folded internal fabric of small amphibole, chlorite and quartz grains, whereas texturally zoned clinozoisite (1–1.5 mm in size) includes only small amphibole grains. The matrix is mainly made of amphibole (mainly 0.3 mm in size), chlorite, albite, quartz and titanite.

Orthogneiss (Additional Fig. 1c): Albite and K-feldspar exhibit 0.5 to 1 mm large porpyphroblasts, which bear many inclusions (mainly quartz and sericite). The matrix comprises quartz and feldspar and a low amount of white mica and chlorite flakes.

Porphyroblastic albite-paragneiss (Additional file 1: Figure S1a, b, e): The porphyroblastic albite-paragneiss represents the most common rock type and several samples have been investigated. In general, these rocks, e.g. sample WW-21, comprise ca. 40 percent xenomorphic ovoid, several mm large albite porphyroblasts, which always have an internal foliation different from the external one. The inclusions (size ca. 0.05–0.1 mm) are white mica, quartz, albite, chlorite, epidote, titanite, allanite, opaque minerals (e.g., ilmenite), zircon, apatite and rare garnet. The matrix consists of dominantly ca. 0.3 mm long chlorite flakes, well annealed quartz with triple junctions and straight grain boundaries, albite, and few biotite grains.

Dark-colored porphyroblastic albite paragneiss: It consists of albite, garnet, quartz, white mica, and chlorite. Albite porphyroblasts (ca. 0.5–1 mm in size) contain inclusions of quartz, albite, and white mica. The

Table 1 Studied samples, their locations, mineralogy and microfabrics

Variegated Wechsel Gneiss Complex						
		Latitude (N)	Longitude (E)	Elevation (m)	Mineralogy	Microfabric
Magmatic protoliths						
WW-15A–D	Greenschist, albite-epidote–amphibolite	47° 27′ 50.80″	15° 54′ 57.30″	694	Albite, chlorite, amphibole, epidote, quartz, garnet, opaque ores, ± white mica	Amphibole-bearing greenschist with albite porphyroblasts
WW-20A–D	Epidote–amphibolite	47° 27′ 32.08″	15° 54′ 46.02″	582	Albite, amphibole, chlorite, opaque ores, quartz	Well foliated epidote amphibolite with albite porphyroblasts
WW-26A	Epidote amphibolite	47° 26′ 33.62″	16° 02′ 44.05″	626	Amphibole, clinozoisite, garnet, chlorite, albite, quartz, titanite	Massive fabric with clinozoisite and garnet porphyroblasts bear many inclusions
WW-27	Orthogneiss	47° 27′ 49.86″	16° 02′ 43.59″	581	Albite, K-feldspar, quartz, white mica, chlorite	Porpyhroblastic fabric with many inclusions in PB
Sedimentary protoliths						
WW-19	Quartzite	47° 27′ 54.20″	15° 55′ 07.03″	658	Quartz, sericite, zircon, opaque minerals	Well annealed quartz fabric, grain boundary migration
WW-16A	Dark coloured paragneiss	47° 27′ 50.80″	15° 54′ 55.27″	679	Albite, garnet, quartz, white mica, chlorite	Albite porphyroblasts, which bear many inclusions of quartz, albite, white mica. Matrix with white mica, chlorite, quartz and albite
WW-21	Porphyroblastic albite-gneiss (Garnet-chlorite schist)	47° 27′ 49.86″	15° 56′ 46.41″	767	Albite, chlorite, quartz, epidote, titanite, white mica, opaque minerals	Porphyroblastic fabric. Matrix consists of mainly chlorite flakes, then quartz, albite, biotite
WW-25A	Albite gneiss	47° 26′ 43.99″	16° 01′ 34.49″	662	Albite, quartz, K-feldspar, sericite, garnet, white mica, ilmenite	Two types of small feldspar: (1) inclusion-free; (2) with many sericite and quartz inclusions. Matrix with quartz, albite, K-feldspar
Wechsel Phyllite Unit						
WW-31	Metatuffite	47°35′09.82″	15°51′53.87″	948	Quartz, some ovoid plagioclase, chlorite, white mica, opaque ores	Two-stage fabric with a metamorphic foliation and a late-stage pressure-solution cleavage
WW-32	Chlorite-rich metatuffite	N 47° 35.158′	E 15° 51.741′	1026	Quartz, chlorite, plagioclase, opaque ores	Layered with thin quartz-rich layers and thick chlorite-rich layers
WW-33	Feldspar-rich metatuff	47° 35′ 09.82″	15° 52′25.40″	1141	Feldspar/plagioclase, quartz, chlorite, epidote, opaques	All grains with a similar size: 0.05–0.1 mm, feldspar-quartz + chlorite
WW-34A	Feldspar-rich metatuffite	47° 32′ 03.88″	15° 51′ 44.97″	968	Quartz, plagioclase, chlorite, sericite	Fine-grained (ca. 0.1 mm) and quartz-rich; foliated.

matrix consists of white mica, chlorite, quartz, albite and little graphitic material.

Quartzite: The quartzite contains quartz, sericite, zircon, opaque minerals. The well annealed quartz fabric shows some grain boundary migration (Additional file 1: Figure S1g). Small sericite flakes occur at straight grain boundaries and obviously controlled the size of polygonal quartz grains.

Garnet-chlorite schist: This schist contains plagioclase, quartz, chlorite, epidote, garnet, opaque ore minerals. All grains have a similar size of 0.05–0.1 mm.

3.2 Microfabrics of the Variegated and Monotonous Wechsel Gneiss Complexes

The rock fabrics and formation of albite porphyroblasts in albite-porphyroblast paragneisses of both Variegated and Montonous Wechsel Gneiss Complexes

allow distinguish several stages of mineral growth (Additional file 1: Fig. S1a, b, e). On several samples of albite-porphyroblast gneiss, preliminary electron microprobe analyses were performed, too (data not shown). The mineral assemblage M1 includes the pre-porphyroblastic inclusions within albite porphyroblasts, which include quartz, both phengitic and paragonitic mica (as also observed by Müller et al. 1999), too, garnet, ilmenite, apatite and zircon, and sometimes graphitic material. Garnet shows two growth stages, with a bell-shaped spessartine-rich core and spessartine-poor but a grossular-rich rim.

The stage M2 includes albite porphyroblasts, quartz, white mica, chlorite and ilmenite, and garnet, garnet could be preserved from stage M1. These minerals are often in textural equilibrium, particularly well visible on recrystallized, strain free quartz and chlorite. Mineral assemblages of stage M3 developed mainly along local shear zones characterized by elongated quartz, fine sericite and chlorite. Finally, it has to be mentioned that subordinate garnet is common in the central southern and eastern sectors of the Variegated and Monotonous Wechsel Gneiss Complexes, matched in mafic rocks by the presence of amphibole and epidote/clinozoisite in the eastern part but no amphibole in the northwest. Consequently, a gradient with increasing P–T conditions from NW to SE can be envisaged.

3.3 Wechsel Phyllite Unit

It has to be noted that the rocks of the Wechsel Phyllite Unit lack the albite porphyroblasts and therefore no polyphase mineral growth fabric can be observed. Many rocks of the Wechsel Phyllite Unit show alternating layering with often fine-grained feldspar and feldspar/quartz layers alternating with chlorite-rich ones. Metatuffite and chlorite-rich metatuffite from the Lower Wechsel Phyllite Unit contain only small grains of a similar size, 0.05–0.1 mm (Additional file 2: Figure S2a, b). The mineral assemblage includes feldspar/plagioclase, quartz, and variable amounts of chlorite, sericite and opaque ore minerals. Some of the samples show alternating thin quartz-rich layers and thick chlorite-rich layers. Structurally, they contain a two-stage fabric with a metamorphic foliation S_1 and a late-stage pressure-solution cleavage S_2, which is often perpendicular to S_1 (Additional Fig. 2a).

One sample (WW-33) is a feldspar-rich metatuffite from the basal part of the Upper Wechsel Phyllite Unit and contains mainly feldspar/plagioclase, quartz, chlorite, epidote, opaque ore minerals, all with similar sizes of 0.05–0.1 mm.

4 Analytical methods

4.1 U–Pb dating analytical methods

Zircons from two representative magmatic samples (WW-26A, epidote–amphibolite; WW-27A, a leucocratic orthogneiss), and from metasedimentary albite-paragneisses (samples WW-16, WW-21, WW-23, WW-25) and a quartzite sample (WW-19A) from the Variegated Wechsel Gneiss unit were dated by the U–Pb method. From the Lower (samples WW-31A, WW-32A, WW-34A) and Upper Wechsel Phyllite Fms. (WW-33A), four plagioclase-rich metatuffaceous samples were dated.

Zircon grains were extracted from samples using conventional density and magnetic separation techniques at the Yuneng Mineral Separation Company, Hebei Province. Over 500 zircons were handpicked under a binocular microscope, then mounted in epoxy resin and polished until the grain centers were exposed. To remove any lead contamination, the surface was cleaned using 3% HNO_3 prior to analysis. In order to characterize internal structures and to choose potential target sites for U–Pb dating, cathodoluminescence (CL) images were obtained using a Mono CL3 + microprobe. For classification of zircon textures and geochemical properties, we follow Corfu et al. (2003), Hoskin and Schaltegger (2003) and Harley et al. (2007).

Measurements of U, Th, and Pb isotope data and trace element compositions of zircons were conducted using a laser ablation-inductively coupled plasma–mass spectrometer (LA-ICP-MS) at the Beijing Createch Testing Technology Co., Ltd. Detailed operating conditions for the laser ablation system and the MC-ICP-MS instrument and data reduction are the same as described by Hou et al. (2009) based on the methodology of Yuan et al. (2004). Laser sampling was performed using a 193 nm laser ablation system. A 24 μm-spot size was adopted in this study with a laser repetition rate of 6 Hz and energy density up to 6 J/cm^2. An Agilent 7500 ICP-MS instrument was used to acquire ion-signal intensities. Helium was applied as a carrier gas. Each analysis incorporated a background acquisition of approximately 15–20 s (gas blank) followed by 45 s data acquisition from the sample. Off-line raw data selection and integration of background and analytical signals, and time-drift correction and quantitative calibration for U–Pb dating was performed by ICPMSDataCal (Liu et al. 2010).

Zircon GJ-1 was used as external standard for U–Pb dating and was analyzed twice every 5–10 analyses. Time-dependent drifts of U-Th–Pb isotopic ratios were corrected using a linear interpolation (with time) for every 5 to 10 analyses according to the variations of GJ-1 (i.e., 2 zircon GJ-1 + 5 to 10 samples + 2 zircon GJ-1) (Liu et al. 2010). Uncertainty of preferred values for the external standard GJ-1 was propagated to the ultimate results

of the samples. In all analyzed zircon grains the common Pb correction was not necessary due to the low signal of common ^{204}Pb and high $^{206}Pb/^{204}Pb$ ratios. U, Th and Pb concentrations were calibrated by NIST 610. Concordia diagrams and weighted mean calculations were made using Isoplot/Ex_ver3 (Ludwig 2012).

For time-scale calibration, we use the most recent version (2020/01) of the ICS International Chronostratigraphic Chart (Cohen et al. 2013).

4.2 Geochemical methods

The major and trace element compositions were determined by X-ray fluorescence (XRF-1800; Shimadzu) on fused glasses and inductively coupled plasma mass spectrometry (Agilent 7500ce) at Beijing Createch Test Technology Co. Ltd. Prior to analysis, all samples were trimmed to remove weathered surfaces before being cleaned with deionized water and crushed to 200 mesh in an agate mill. Sample powders (~40 mg) were digested using HNO_3 and HF acids in Teflon bombs. Loss-on-ignition (LOI) values were measured after heating 1 g of sample in a furnace at 1000 °C for several hours in a muffle furnace. The precision of the XRF analyses is within ± 2% for the oxides greater than 0.5 wt% and within ± 5% for the oxides greater than 0.1 wt%.

Sample powders (about 50 mg) were dissolved in Teflon bombs using a HF + HNO_3 mixture for 48 h at about 190 °C. The solution was evaporated to incipient dryness, dissolved by concentrated HNO_3 and evaporated at 150 °C to dispel the fluorides. The samples were diluted to about 100 g for analysis after being redissolved in 30% HNO_3 overnight. An internal standard solution containing the element Rh was used to monitor signal drift during analysis. Analytical results for USGS standards (Jochum et al. 2005) indicated that the uncertainties for most elements were within 5%.

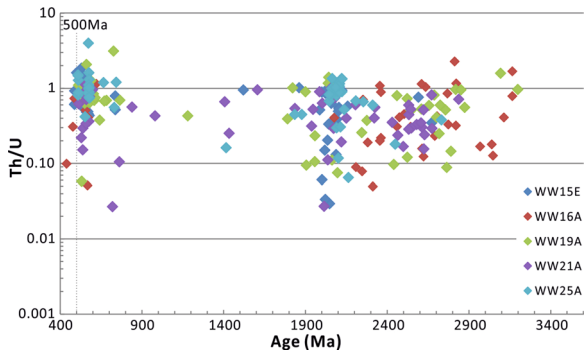

Fig. 6 Th/U ratios vs. age of studied samples from the Variegated Wechsel Gneiss Complex

5 Results

In the following description of detrital zircons in metasedimentary rocks, we use the 95-105 percent limit of concordance although most data are between 98 and 102 percent. Following Andersen (2002), we use the $^{208}Pb/^{238}U$ age for ages < 1.0 Ga, and the $^{207}Pb/^{206}Pb$ age for ages > 1.0.

5.1 Magmatic protoliths of the Variegated Wechsel Gneiss Complex

Analytical results of U–Pb zircon dating on rocks of the Variegated Wechsel Gneiss Complex are given in Additional file 3: Table S1. Sample WW-26A is an epidote–amphibolite, from which 40 zircon grains were studied. Many grains are broken, some are euhedral, some are partially resorbed (Fig. 5). Some grains have small bright rims, which postdate breaking. Many grains are internally uniform and grey in CL images, other grains bear

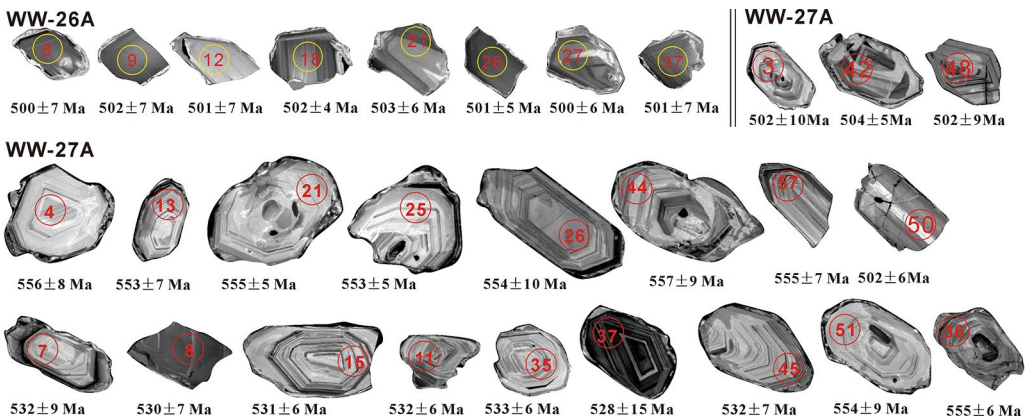

Fig. 5 Representative cathodoluminescence images of zircons of magmatic rocks from the Variegated Wechsel Gneiss Complex

an oscillatory zoning. The U contents range between 268 and 732 ppm. The Th/U ratios are between 0.89 and 2.33, most grains scatter at ca. 0.9 to 1.1 indicating a magmatic origin of these zircons (Fig. 6). 35 of them gave a well-defined intercept age of 501.3 ± 2.3 Ma (MSWD = 0.025) (Fig. 7a). No inherited grains were found in this sample.

Sample WW-27A is an orthogneiss with often euhedral zircon grains, which show an oscillatory zoning and sometimes inclusions of minerals like euhedral apatite. Some grains have a dark rim around zoned cores (Fig. 5). The Th/U ratios are between 0.85 and 2.13, with a majority around 1.0 (Fig. 6). Sixty grains were measured and fifty-five of them are concordant (Fig. 7b). All grains together give a discordia with a lower intercept age of 523 ± 21 Ma and an upper intercept age of 1513 −90/+91 Ma. However, the youngest four grains are internally very consistent at 502.9 ± 6.5 Ma (Fig. 7d), show an oscillatory zoning (Fig. 5) and have Th-U ratios

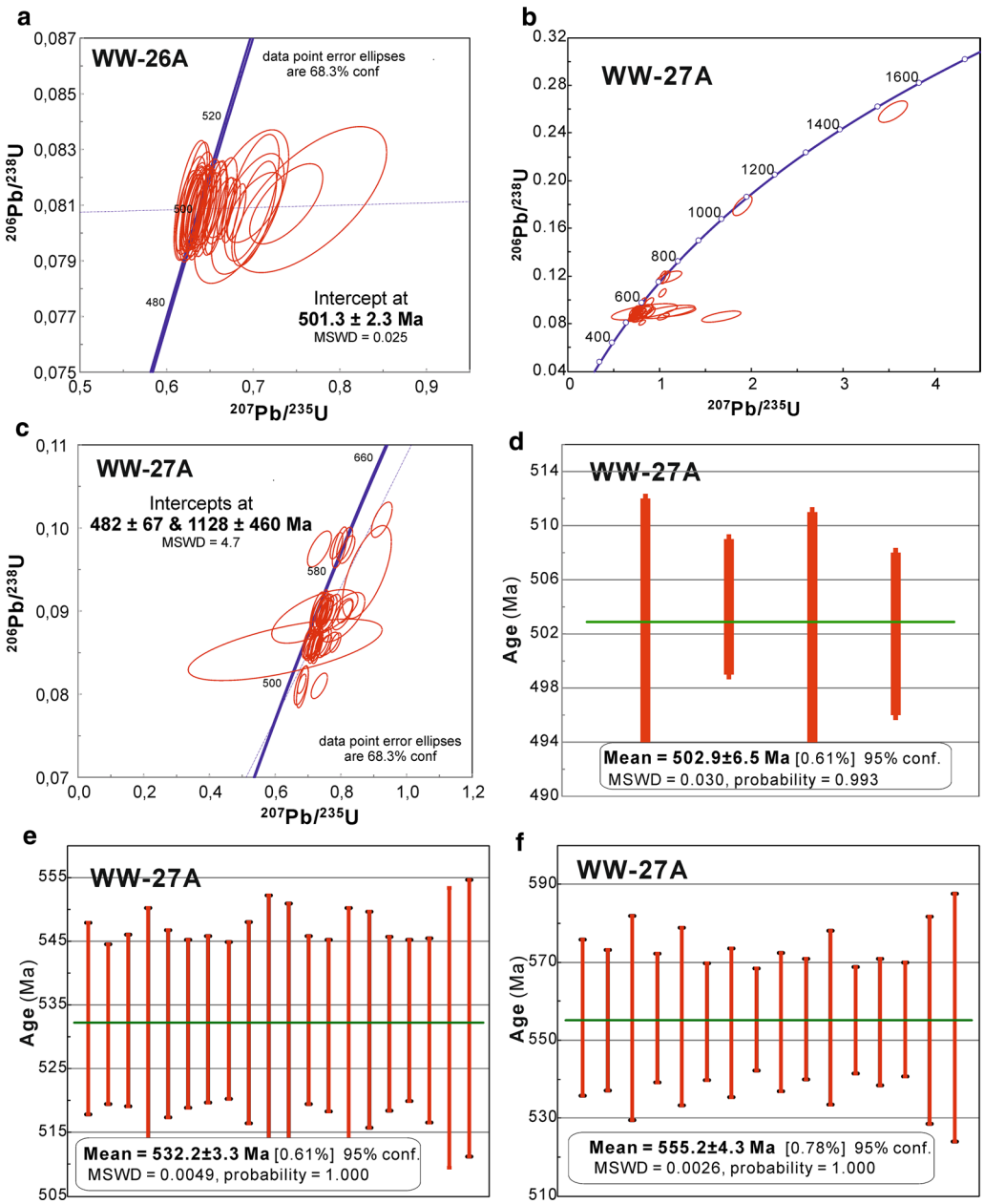

Fig. 7 LA-ICP-MS U–Pb zircon concordia diagrams and $^{206}Pb/^{238}U$ weighted mean age of various age populations of magmatic rocks from the Variegated Wechsel Gneiss Complex

of 1.02 to 2.04 (Additional file 3: Table S1) classifying them as magmatic zircons. However, it must be noted that these zircon grains are slightly discordant (Fig. 7c). Twenty grains are at 532.2 ± 3.3 Ma, and another group with 16 grains at 555.2 ± 4.3 Ma (Fig. 7e, f). Thus, the youngest grains with 502.9 ± 6.5 Ma should represent the age of magmatism reworking two stages of older magmatic events (Fig. 7c, d). Leucocratic orthogneisses are known to include a high proportion of inherited zircons as a relict of the melting process (e.g., Shakerardakani et al. 2020).

5.2 Metasedimentary protoliths of the Variegated Wechsel Gneiss Complex

Representative CL images of zircons from all metasedimentary samples are shown in Fig. 8, the analytical results are given in Additional file 3: Table S1 and are graphically shown in Fig. 9. The zircons are often rounded (Fig. 8). Cl images of many grains show an oscilliatory zoning or a more uniform pattern. Sometimes, grains show a dark rim. The U contents of all four investigated metasedimentary rocks of the Variegated Wechsel Gneiss Complex vary between 37 and 3455 ppm, with a clear majority between 90 and 490 ppm. Th/U ratios vs. age are shown in Fig. 5. All Th/U ratios are higher 0.1 beside a few scattered values, mostly with Early Proterozoic ages (Fig. 5). This implies that most grains have a magmatic origin.

Sample WW-19A is a pure quartzite with generally well rounded zircons, often with a very thin dark rim. 80 grains were studied and 74 of them are (sub-) concordant. From the concordant grains, the youngest age is 513 ± 10 Ma, the oldest 3161 ± 17 Ma. Major age populations occur at 570 Ma, 1.2 Ga, 2.15 Ga, 2.5 Ga and 2.75 Ga (Fig. 9e, f).

Sample WW-16A is a dark-coloured albite-paragneiss, from which 60 grains were studied, 57 of them are (sub-) concordant. From the concordant grains, the youngest age is 544 ± 10 Ma, the oldest 3032 ± 5 Ma. The age population at 560 Ma is dominating. Further large populations occur at 2.25 and 2.65 Ga (Fig. 9g, h).

Sample WW-21A is a garnet-chlorite schist with mostly rounded zircons, which also bear an oscillatory zoning in the core and a thin grey rim in CL images. Some grains are subhedral. The U contents range from 31.7 to 1619 ppm. 80 grains were studied, 77 grains are (sub)concordant. Of the concordant grains, the youngest age is 487 ± 8 Ma (97% concordancy), the oldest 2931 ± 13 Ma (Fig. 9c, d). Major age populations are at 550.4 ± 4.6 Ma (with subhedral grains often exhibiting an oscillatory zoning), 2027 ± 21 Ma and 2588 ± 20 Ma (Fig. 9k–m).

Sample WW-25A is an intermediary albite-gneiss with heterogeneous zircon populations in CL images. 40 grains were studied, 26 of them are (sub)concordant. The youngest age is 509 ± 7 Ma, the oldest 2731 ± 13 Ma (Fig. 9a, b). Major age populations are at 577.4 ± 4.0 Ma, and at 2287 ± 8 Ma (Fig. 9i, j).

5.3 Summary of protolith ages of the Variegated Wechsel Gneiss Complex

The Variegated Wechsel Gneiss Unit contains magmatic rocks (greenschists, acidic orthogneisses) with U–Pb

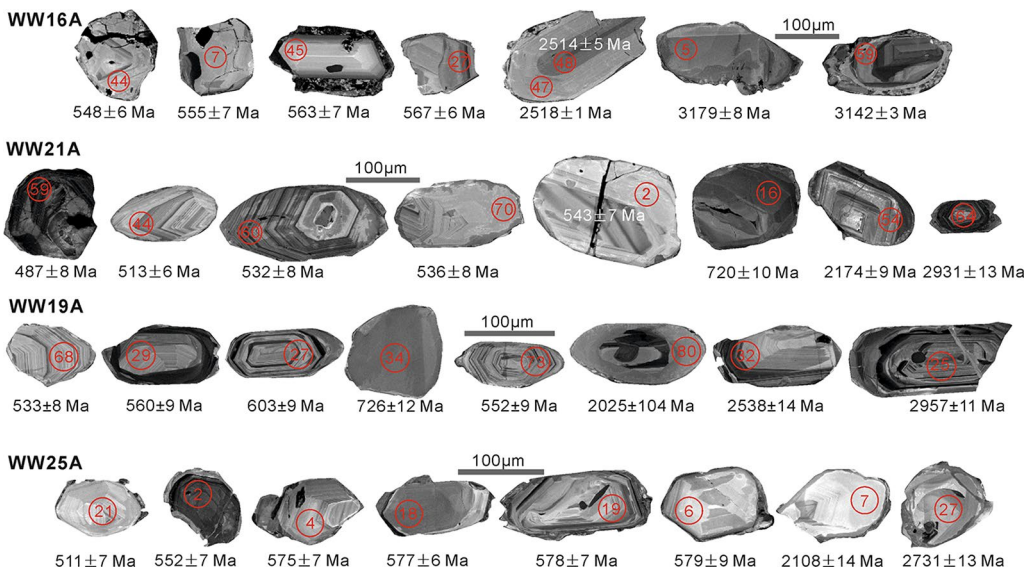

Fig. 8 Representative cathodoluminescence images of zircons of metasedimentary rocks from the Variegated Wechsel Gneiss Complex

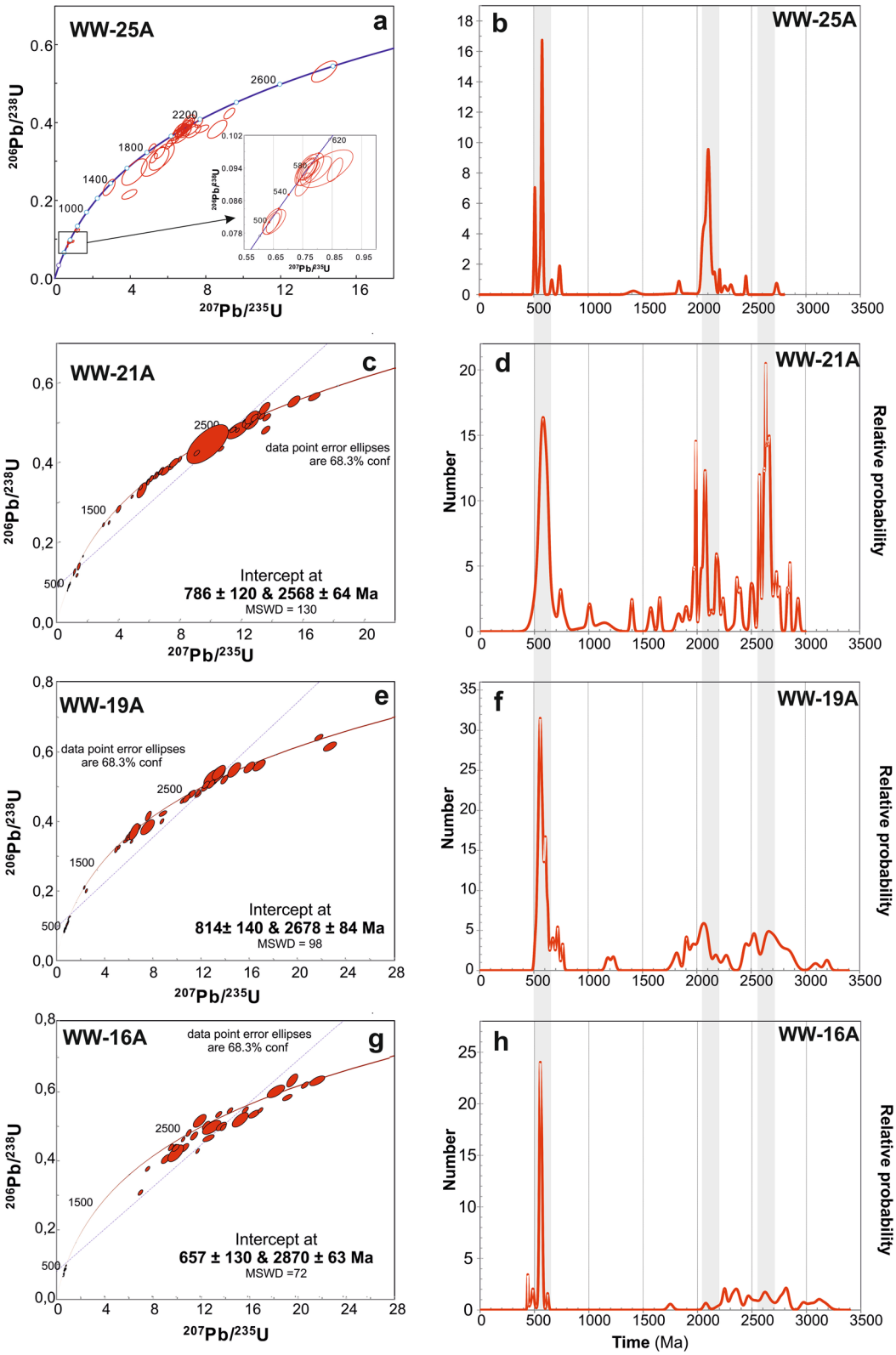

Fig. 9 LA-ICP-MS U–Pb zircon concordia diagrams and $^{206}Pb/^{238}U$ weighted mean age of representative age populations of metasedimentary rocks from the Variegated Wechsel Gneiss Complex

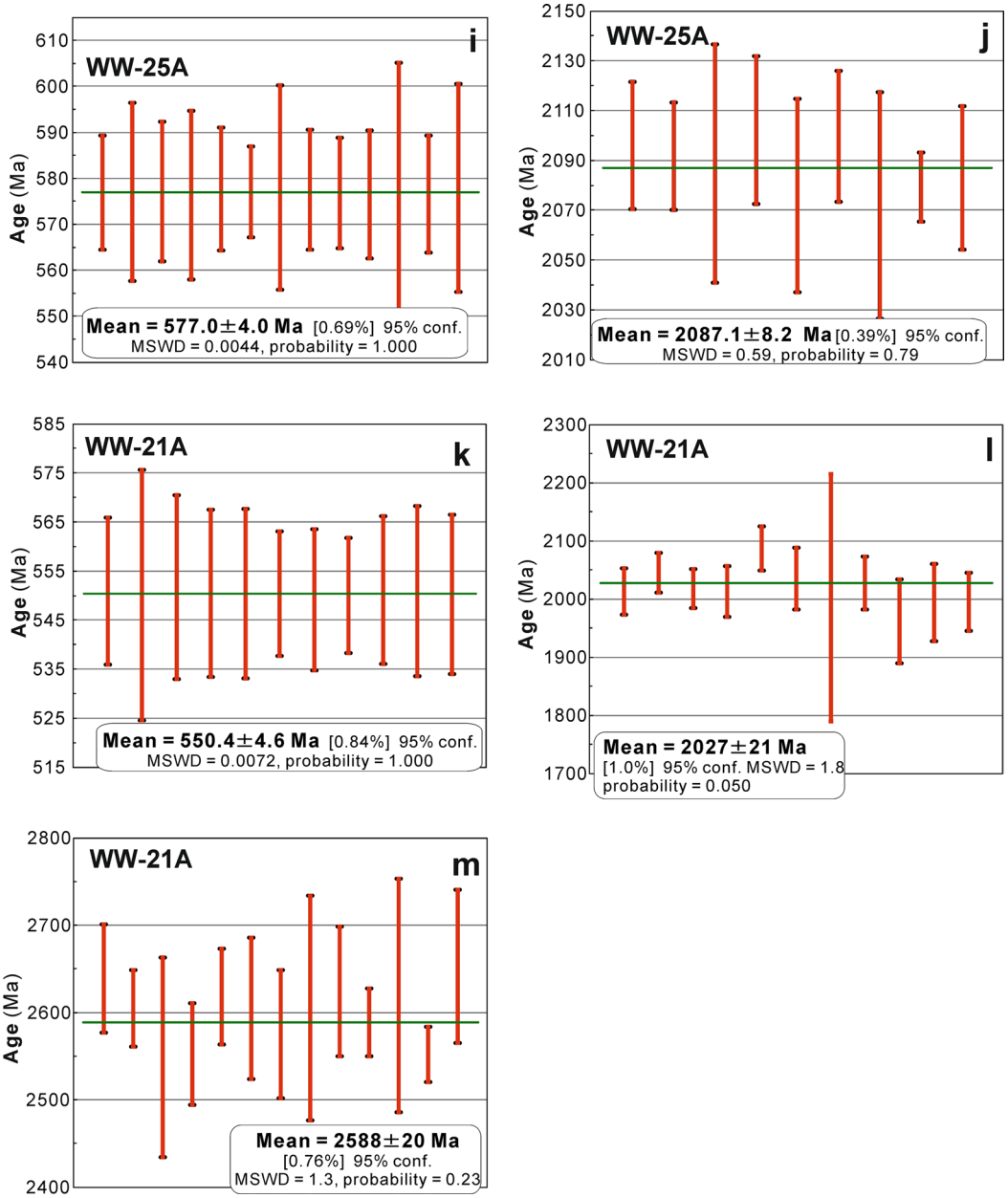

Fig. 9 continued

zircon ages of 500 Ma and 523 Ma. In paragneisses and quartzite, the detritus is dominated by several age groups that include euhedral zircons of at ca. 500 Ma, 550 Ma and detrital components of ca. 1.9–3.2 Ga, with a pronounced maximum of ca. 2.1 Ga.

5.4 Detrital ages of the Wechsel Phyllite Unit

Representative CL images of all metasedimentary samples from the Wechsel Phyllite Unit are shown in Fig. 10, the analytical results are presented in Additional file 4: Table S2, the Th/U ratio vs. age diagram is shown in Fig. 11, and the dating results are graphically shown in Figs. 12 and 13. The CL images show euhedral and subhedral grains with an oscillatory zoning. Other grains are rounded and have a uniform internal texture or show sector zoning. A few grains seem partially resorpt as embayments show (Fig. 10, spot 50 of sample WW-33A). The U contents range between 31 and 2440 ppm with a majority between 60 and 240 ppm. Except a significant Early Proterozoic age

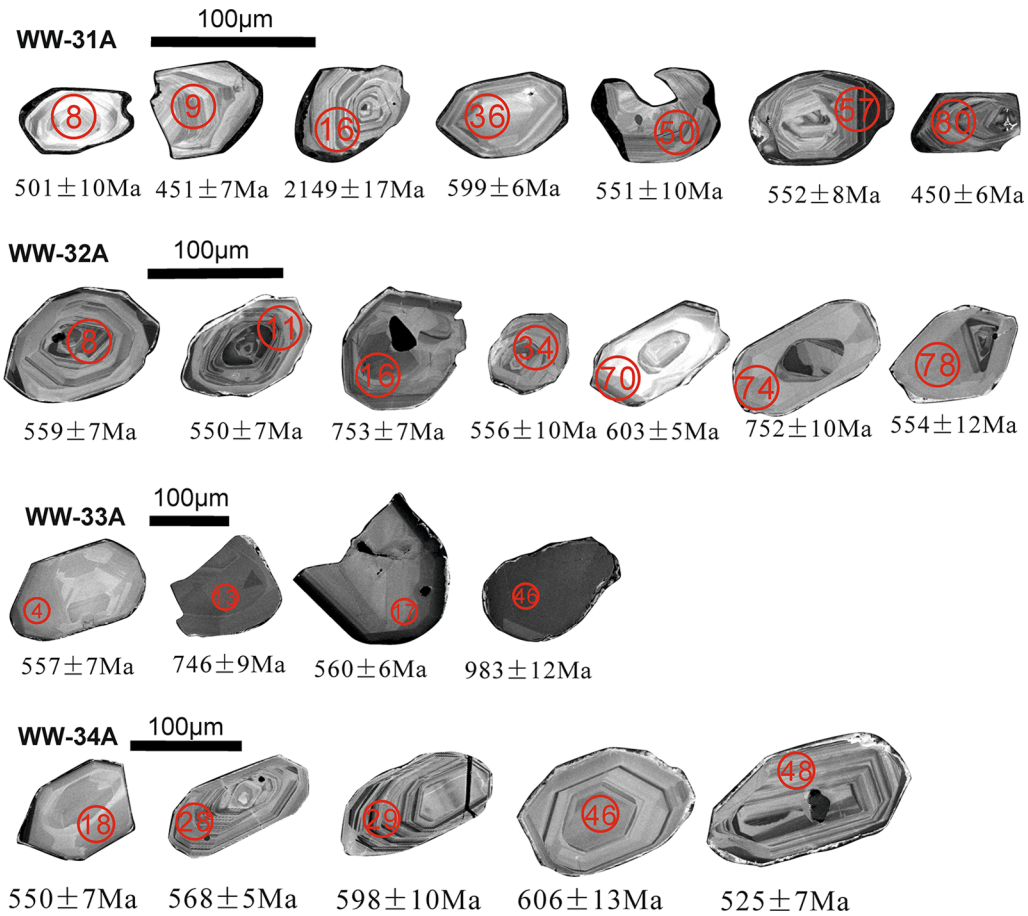

Fig. 10 Representative cathodoluminescence images of zircons of metatuffites from the Wechsel Phyllite Unit

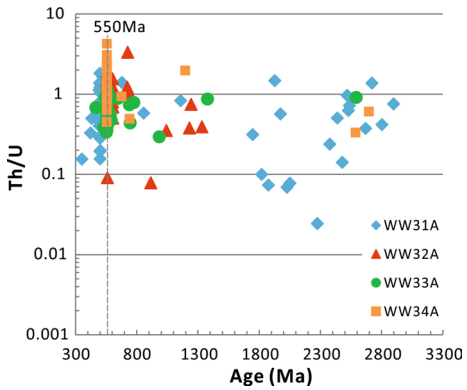

Fig. 11 Th/U ratios vs. age of studied samples of the Wechsel Phyllite Unit

population of sample WW-31A, all other Th/U classify these grains as magmatic (Fig. 11).

From sample WW-31A, a quartz-rich, but metatuffaceous rock with mostly euhedral zircons, 80 grains were measured, from which 59 are concordant within 95 and 105 percent. Three (sub)concordant euhedral grains are at 450 Ma (Th/U = 0.45–0.72 indicating their magmatic origin; Fig. 11), a major age population (16 grains) gives a weighted mean age of 500.5 ± 4.6 Ma (16 grains), a population of 10 grains an age of 520.9 ± 5.5 Ma, another one an age of 550.3 ± 5.7 Ma (9 grains) (Fig. 12a, c–e). The oldest grain has an age of 2672 ± 11 Ma.

Sample WW-32A is a chlorite-rich metatuffite with mostly euhedral and subeuhedral zircons, 80 grains were measured, from which 75 are concordant within 95 and 105 percent. Three euhedral grains show an age of 522 Ma, the majority with 34 grains gives a weighted mean age of 558.3 ± 2.5 Ma (Fig. 12b, f). Other distinct age groups are at 603.5 ± 6.5 Ma (10 grains) and 726.8 ± 8.4 Ma (6 grains) (Fig. 12g, h). The oldest grain has an age of 2908 ± 11 Ma.

Sample WW-33 is a feldspar-rich metatuff, from which 60 grains were measured, of which 50 grains are (sub) concordant (Fig. 13a, b). The grains are mainly euhedral and display an oscillatory zoning and some are patchy,

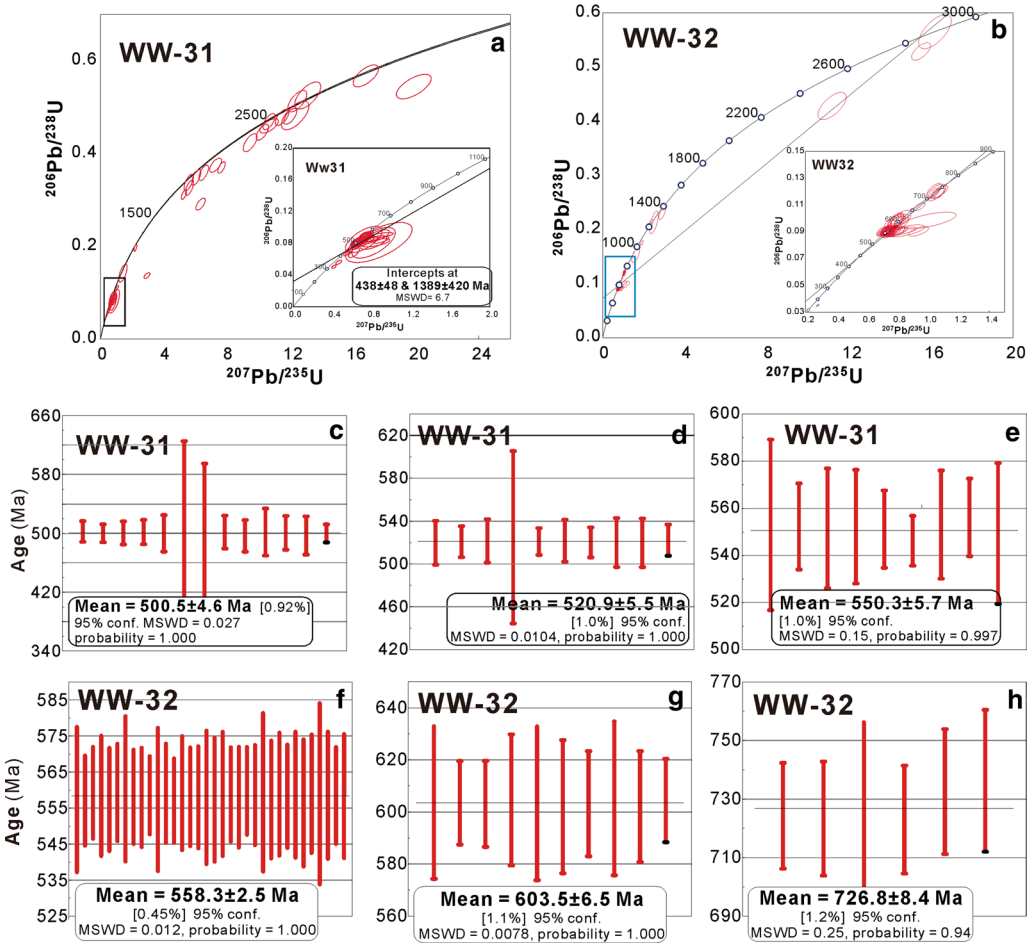

Fig. 12 LA-ICP-MS U–Pb zircon concordia diagrams and $^{206}Pb/^{238}U$ weighted mean age of representative age populations of from the Wechsel Phyllite Unit (samples WW-31 and WW-32)

other grains have some small inclusions (Fig. 10). Other grains are patchy and some seem partially resorbed. Some grains show a thin bright rim. Concordia calculations give no meaningful results (Fig. 13a, b) The lower intercept age is at 569 ± 34 Ma (Fig. 13a). Dominating is a population, which gives $^{206}Pb/^{238}U$ weighted mean age of 556.5 ±2.3 Ma (Fig. 13e). One grain is younger, 464.8 ± 4.7 Ma (Th/U = 0.68), a few subconcordant grains are older: 591.4 ± 4.6 Ma, 644.1 ± 10.4 Ma, 740.1 ± 7.8 Ma, 746.4 ± 9.9 Ma, 775.7 ± 6.9 Ma, 1376 ± 14.5 Ma and 2861 ± 5 Ma (this one with a concordancy of 94%).

Sample WW-34A is a feldspar-rich metatuffite and bears many rounded zircon grains, but also many euhedral ones (Fig. 10). Most grains scatter at ca. 550 Ma and inly few grains are older or younger (Fig. 13c, d). The weighted mean age of 52 grains is at 555.3 ± 2.4 Ma (Fig. 12f). Few other grains have ages of 493 ± 18 Ma (96% concordance), 606 ± 13 Ma (93% concordance), 633 ± 15 Ma, 1336 ± 17 Ma Ma, 2965 ± 9 Ma (94% concordance), 2994 ± 11 Ma.

Consequently, the four samples of the Wechsel Phyllite Unit include similar zircon age populations although the relative proportions of the age populations are variable. The dominant age group is at 555 to 560 Ma (Late Ediacaran). A small age population includes the youngest zircons with ages of 450 to 456 Ma. Major age populations are at 500 Ma, 520 Ma, 560 Ma, 600 Ma and 753 Ma. The age group at 450 to 456 Ma implies that the depositional age is equal or younger than 450 Ma (Katian of Upper Ordovician; Cohen et al. 2013).

5.5 Preliminary geochemical characterization of mafic rocks

The chemical composition of representative metabasaltic rocks (greenschists and epidote-amphibolites with albite porphyroblasts) were investigated from two locations

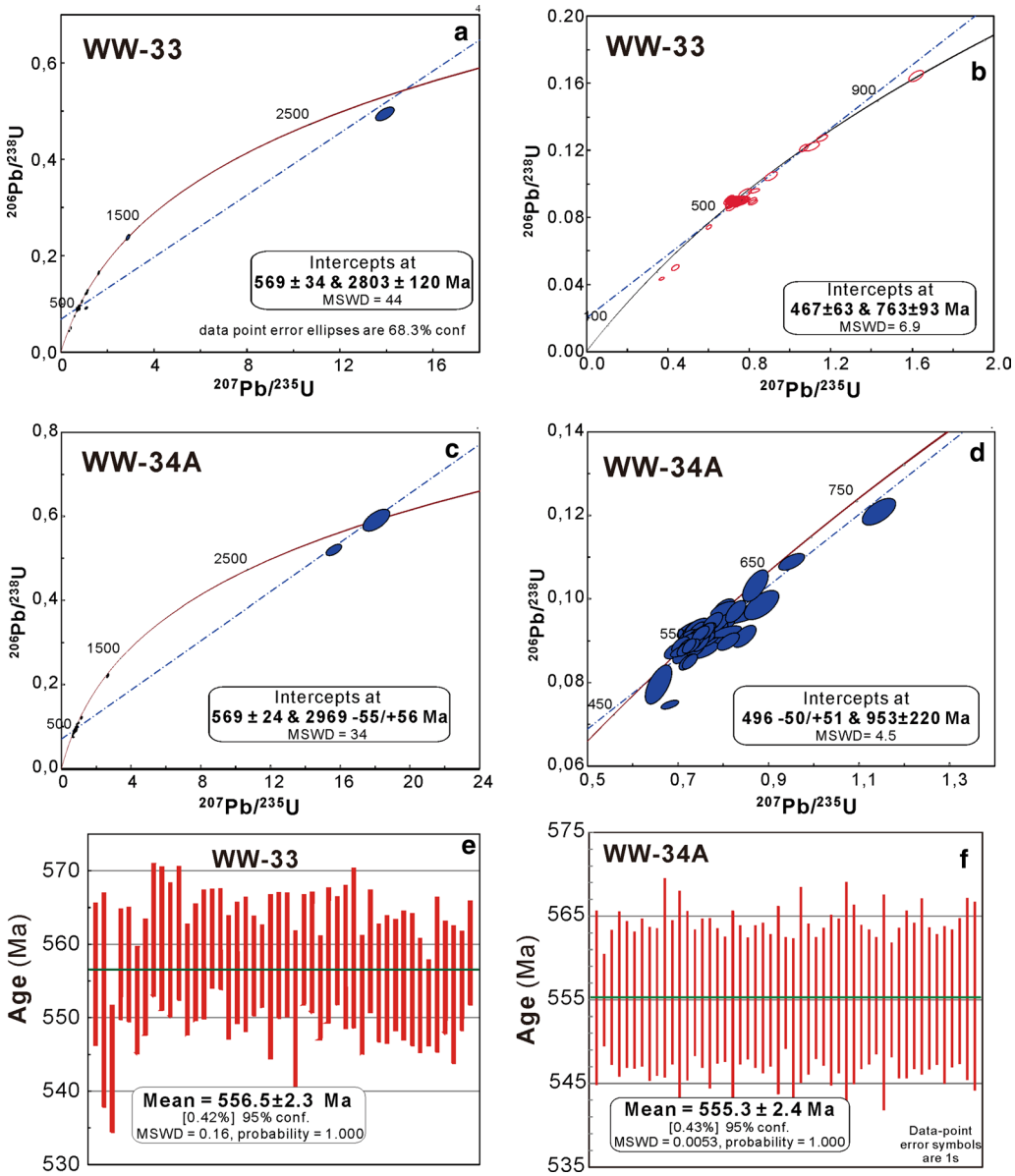

Fig. 13 LA-ICP-MS U-Pb zircon concordia and age distribution diagrams and $^{206}Pb/^{238}U$ weighted mean age of representative age populations of from the Wechsel Phyllite Unit (samples WW-32 and WW-34)

(Table 2 with results). Four and six samples were collected in these two localities with visible differences in texture and mineral proportions. Unfortunately, the rocks of these locations did not contain zircons, so their age is not constrained. From the geochemical composition, the samples from the location WW-15 are internally relatively homogeneous, whereas those of location WW-20 show a significant variation in their geochemical patterns (Figs. 14, 15a, b). The loss of ignition (LOI) of six samples from location WW-15 is consistently at ca. 5 wt%, from samples at location WW-20 at ca. 1 wt% with two exception at 2.13 and 2.84 wt%. The samples from location WW-15 have high chlorite contents of ca. 40–50 modal percent. The SiO_2 contents of the samples vary between 52.30 and 53.00 wt%, in location WW-20 between 48.51 and 53.38 wt%. The major difference between samples of both locations is the higher CaO content (7.35–9.85 wt%) and lower MgO contents (5.52–6.86) in samples from WW-20 compared to WW-15 (1.54–2.65 wt%) and (7.66–9.02 wt%). The NaO content is lower in location WW-15 (3.00–3.67 wt%) than in WW-20 (3.90–4.31 wt%).

Table 2 Geochemical data

Sample	SiO_2	TiO_2	Al_2O_3	Fe_2O_3	MnO	MgO	CaO	Na_2O	K_2O	P_2O_5	LOI			
WW15A	53.00	1.20	15.84	11.53	0.09	9.02	1.54	3.00	0.07	0.17	5.24			
WW15B	52.36	1.26	16.66	11.38	0.09	7.66	2.65	3.37	0.09	0.18	4.83			
WW15C	52.30	1.24	16.54	11.37	0.09	7.74	2.55	3.36	0.08	0.16	4.79			
WW15D	52.36	1.22	16.64	11.19	0.09	7.86	2.23	3.61	0.08	0.16	4.77			
WW20A	53.38	1.33	15.68	10.19	0.19	5.52	7.35	4.07	0.83	0.18	1.10			
WW20B	51.01	1.36	15.84	11.19	0.19	6.08	8.32	3.90	0.59	0.18	0.98			
WW20C	52.21	1.34	15.85	10.63	0.19	5.99	7.75	4.16	0.68	0.19	1.11			
WW20D	50.58	1.40	14.56	11.96	0.21	6.48	8.78	4.20	0.28	0.14	1.35			
WW20E	50.04	1.33	14.04	11.12	0.19	6.19	9.85	4.10	0.28	0.10	2.84			
WW20F	48.51	1.50	15.79	12.52	0.19	6.86	7.75	4.31	0.30	0.14	2.13			
	Ba	**Rb**	**Sr**	**Zr**	**Nb**	**Ni**	**Co**	**Zn**	**Y**	**Cs**	**Ta**	**Hf**	**Th**	**U**
WW15A	13.4	1.46	70.9	103.9	3.7	189.1	46.07	73.10	25.93	0.07	0.23	2.55	0.89	0.30
WW15B	17.1	2.11	218.7	110.8	3.9	161.3	43.65	65.87	30.32	0.08	0.25	2.71	1.01	0.36
WW15C	16.4	1.95	210.5	109.7	3.9	148.8	44.60	67.31	30.75	0.07	0.24	2.67	0.99	0.34
WW15D	14.0	1.78	166.5	106.8	3.7	146.4	45.33	72.31	28.62	0.10	0.22	2.55	1.03	0.34
WW20A	204.9	25.19	257.3	118.3	4.0	32.4	33.65	85.40	31.23	0.31	0.25	2.97	1.47	0.56
WW20B	154.2	17.88	263.6	128.4	4.0	53.2	35.89	109.49	35.29	0.24	0.26	3.20	1.77	0.63
WW20C	151.8	19.85	269.5	127.3	4.4	32.8	36.24	109.07	33.66	0.23	0.27	3.22	1.63	0.58
WW20D	45.5	4.20	149.0	76.8	2.1	31.5	33.81	72.12	27.94	0.04	0.14	2.03	0.67	0.28
WW20E	48.0	5.79	195.5	81.0	2.5	99.5	39.47	91.19	31.90	0.06	0.17	2.19	0.67	0.31
WW20F	62.6	7.10	222.2	94.5	2.7	76.5	42.55	97.99	34.96	0.10	0.19	2.61	0.86	0.39
	La	**Ce**	**Pr**	**Nd**	**Sm**	**Eu**	**Gd**	**Tb**	**Dy**	**Ho**	**Er**	**Tm**	**Yb**	**Lu**
WW15A	6.99	17.12	2.38	10.71	3.02	1.04	3.82	0.63	4.09	0.84	2.55	0.37	2.44	0.35
WW15B	7.50	18.99	2.63	12.01	3.57	1.51	4.78	0.77	4.80	0.98	2.79	0.39	2.44	0.34
WW15C	7.70	19.43	2.66	12.16	3.51	1.50	4.62	0.75	4.84	0.99	2.85	0.39	2.52	0.33
WW15D	8.04	20.28	2.75	12.53	3.48	1.51	4.37	0.69	4.39	0.89	2.60	0.36	2.28	0.30
WW20A	10.83	26.21	3.59	16.01	4.09	1.32	4.81	0.76	4.77	0.98	2.90	0.41	2.67	0.41
WW20B	12.87	30.76	4.19	18.18	4.55	1.40	5.27	0.84	5.34	1.11	3.28	0.48	3.09	0.47
WW20C	11.52	28.01	3.85	17.02	4.44	1.39	5.17	0.80	5.24	1.08	3.20	0.46	3.01	0.46
WW20D	4.32	11.33	1.72	8.67	2.82	1.01	3.94	0.65	4.28	0.89	2.67	0.37	2.45	0.37
WW20E	4.43	11.74	1.82	9.00	3.02	1.08	4.26	0.72	4.73	1.02	3.04	0.44	2.83	0.43
WW20F	6.27	15.88	2.38	11.69	3.73	1.41	5.08	0.84	5.45	1.13	3.31	0.46	2.97	0.43
	Li	**Be**	**Sc**	**V**	**Mn**	**Cu**	**Ga**	**Mo**	**Sn**	**W**	**Tl**	**Pb**	**Bi**	
WW15A	76.07	0.39	29.81	220.6	673.6	11.00	17.61	0.84	1.28	0.34	0.01	1.62	0.05	
WW15B	66.50	0.41	33.64	235.2	694.4	19.59	19.05	0.74	1.91	0.18	0.02	5.04	0.12	
WW15C	67.29	0.42	33.81	250.8	707.2	20.09	19.17	0.49	1.85	0.23	0.02	4.90	0.11	
WW15D	64.48	0.41	31.31	237.1	681.2	20.83	18.54	0.56	1.54	0.12	0.02	4.13	0.09	
WW20A	12.56	0.60	33.31	280.5	1475.0	5.40	19.11	0.39	1.10	0.08	0.12	6.79	0.03	
WW20B	14.16	0.72	33.69	301.0	1588.8	5.46	21.23	0.78	1.67	0.17	0.08	8.26	0.03	
WW20C	13.68	0.60	35.47	295.6	1571.8	5.02	20.15	0.37	1.27	0.17	0.10	8.92	0.03	
WW20D	11.29	0.39	31.89	247.0	1324.0	19.01	14.44	0.34	1.22	0.01	0.02	2.92	0.04	
WW20E	13.90	0.40	40.19	332.3	1529.1	16.62	17.95	1.33	2.63	0.19	0.03	4.03	0.05	
WW20F	16.26	0.46	46.02	353.4	1454.2	15.04	20.04	0.86	2.37	0.12	0.04	4.13	0.05	

In the trace element discrimination diagram Nb/Y vs. Zr/TiO_2 for volcanic rocks after Winchester and Floyd (1977), all samples plot in the field of basalt respectively andesite (Fig. 14a). In terms of chondrite-normalized REE variation (after Boynton 1984), two patterns can be distinguished: (i) a flat REE pattern with no Eu anomaly,

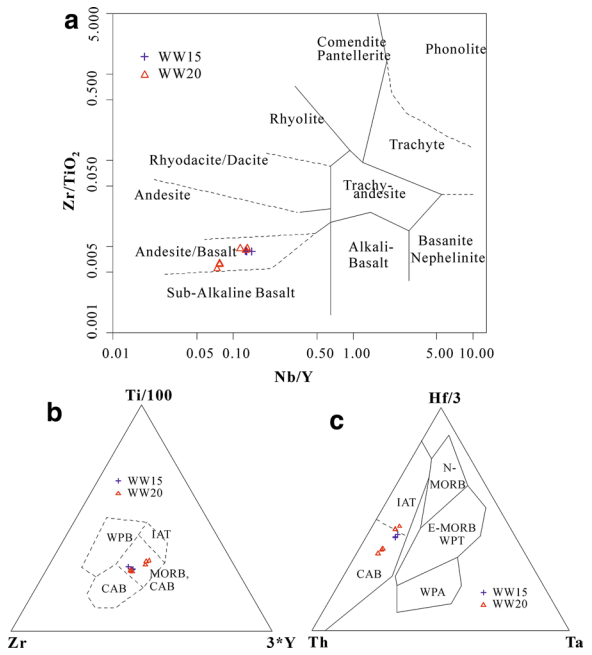

Fig. 14 Trace element geochemical characterization of mafic magmatic rocks from the Variegated Wechsel Gneiss Complex. **a** Characterization of mafic magmatic rocks (after Winchester and Floyd (1977)). **b** Basalt tectonic discrimination of Pearce and Cann (1973). **c** Triangular diagrams of the Th–Hf–Ta system of Wood (1980)

and ii) slightly enriched patterns with a small negative Eu anomaly (Fig. 15a). The REE pattern of samples WW-20 are between these two patterns. In primitive mantle-normalized variation diagrams (Fig. 15b), the samples from WW-15 are depleted in Rb, K, Ba showing the mobility of large-ion lithophile elements, which are not considered, therefore, for interpretation. All investigated samples show a negative Nb anomaly typical for a subduction-related environment, samples from location WW-20 also a small negative Ti anomaly (Fig. 15b). In trace element discrimination diagrams for basalts after Pearce and Cann (1973) and Wood (1980), the mafic rocks plot into the fields of calcalkaline basalts (Fig. 14b, c). In summary, the investigated samples have a calcalkaline affinity and also exhibit some diversity in their composition.

6 Discussion

The first U–Pb zircon ages from the Wechsel basement allow to much better constrain the geological history of that key region of the Alpine basement, which differs in lithology from other Austroalpine basement regions. We first discuss the age and tectonic setting of the Variegated Wechsel Gneiss Complex, then the age of the Wechsel Phyllite Unit, and finally compare the results with other areas of the Eastern Alps.

6.1 Age of the Variegated Wechsel Gneiss Complex

For the age discussion, major age populations and the youngest (sub)concordant U–Pb age of all samples are shown in Fig. 16. The age of the Variegated Wechsel Gneiss Complex is constrained by the Devonian age (ca. 375 Ma) of pressure-dominated metamorphism (Müller et al. 1999) and the age of 501.3 ± 2.3 Ma of the epidote–amphibolite (sample WW-26A) as well as by the youngest magmatic age population (502.9 ± 6.5 Ma) in the orthogneiss (WW-27A). We regard the single subconcordant age of 487 ± 8 Ma of sample WW-21A as not sufficiently significant as formation age, despite the concordancy of 97 percent. At present, it is not clear whether the dated epidote amphibolite and the orthogneiss are intrusions or not, e.g. representing lava flows or metatuffs. The sheet-like character of the orthogneiss overlying a pronounced garnet-micaschist level argues for a volcanic edifice rather than for an intrusion. Metasedimentary rocks carry zircons with the youngest age at

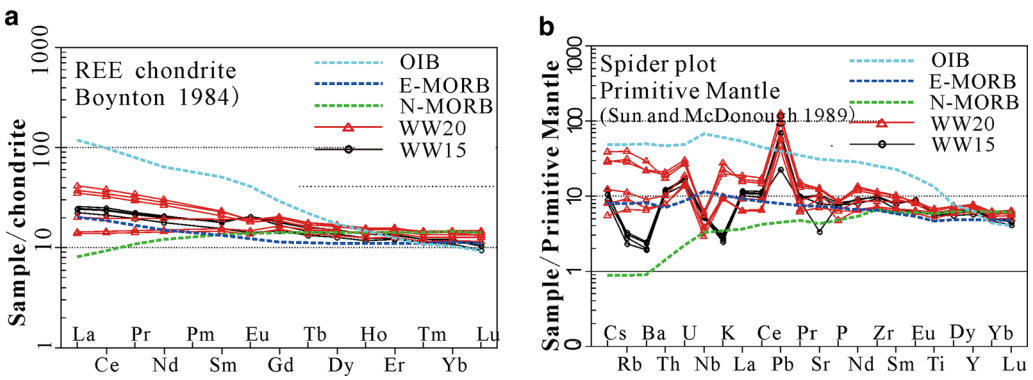

Fig. 15 **a** REE patterns of mafic rocks from the Variegated Wechsel Gneiss Complex. **b** Multi-element variation diagram of mafic rocks from the Variegated Wechsel Gneiss Complex

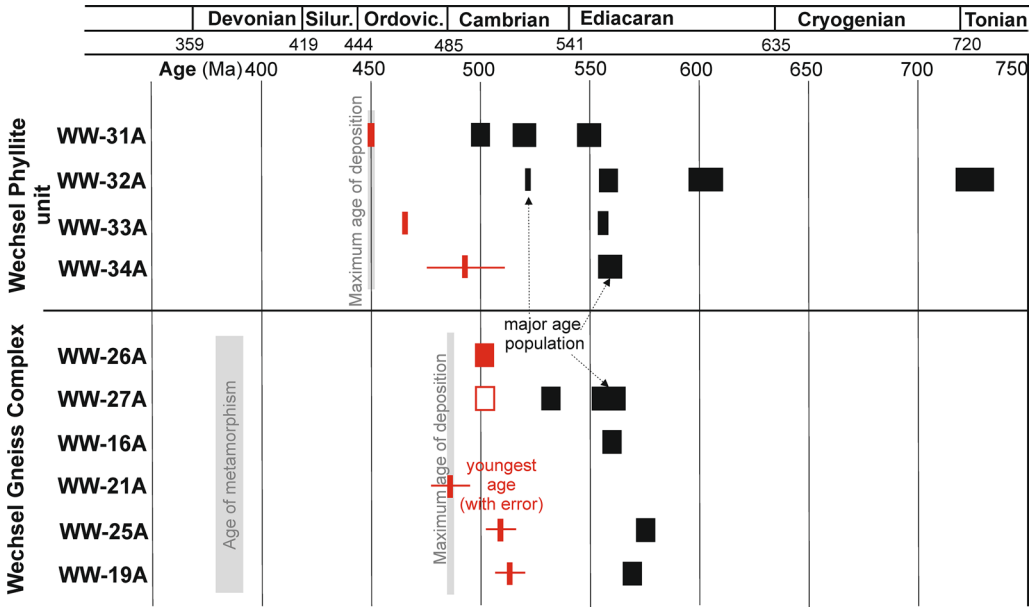

Fig. 16 Overview of U–Pb zircon ages from the Wechsel basement

around 510 Ma (Fig. 16). Together, the observations suggest that the deposition of the metasedimentary rocks of the Variegated Wechsel Gneiss Complex is younger than 510 Ma, between Middle Cambrian (ca. 510 Ma) and Middle Devonian (375 Ma). As the rocks bear a high amount of volcanosedimentary detritus, a subduction-related setting along an active continental margin is the most likely tectonic environment. This subduction-related system shows major magmatic components of ca. 500, 530 and 550–575 Ma.

6.2 Age of the Wechsel Phyllite Unit

The age group at 450 to 456 Ma of two samples implies that the depositional age is equal or younger than 450 Ma (Katian of Upper Ordovician; Cohen et al. (2013) (Fig. 16). As already pointed out by Faupl (1970a), the upper age limit is Early Permian, proven by the superposition of Lower Permian, acidic tuffs bearing clastic sedimentary rocks. In that case, the few 450–456 Ma ages represent volcanic input, as also supported by the richness of plagioclase and chlorite, the age of the Wechsel Phyllite Unit would be Late Ordovician. We envisage this as the most likely age as plutonic rocks of this age are common in the upper part of the Austroalpine nappe complex and contributed to the detritus (Heinrichs et al. 2012; Siegesmund et al. 2007) and also the Southern Alps (Meli and Klötzli 2001; Arboit et al. 2018). The acidic volcanic detritus within these units is ca. 10–15 Ma younger than in the Upper Austroalpine Noric nappe (463 ± 6 Ma) (Söllner et al. 1997; Flajs and Schönlaub 1976) (Eastern and Western Greywacke zone in Fig. 1a). At present, the poor exposure of the northwestern part of the Wechsel window does not allow to fully clarify the relationship between the Monotonous and Variegated Wechsel Gneiss Complexes and the overlying Wechsel Phyllite Unit. As no strongly sheared rocks were found, we tentatively assume a primary relationship. In this case, the Wechsel Phyllite Unit must have an age not older than Famennian in the Late Devonian and older than Permian. As the different potential depositional ages imply significant differences of the tectonic evolution, we propose two hypotheses (see below; Fig. 17), which are called Hypothesis 1 with a Late Devonian to potentially Mississippian age and Hypothesis 2 with a Late Ordovician age, which could be resolved by future research.

6.3 Tectonic model for the evolution of the Wechsel basement

The U–Pb zircon dating of rocks from the Variegated Wechsel Gneiss Complex suggests three major phases of magmatism, dominantly at 550–570 Ma (Ediacaran) and subordinately at ca. 530 Ma and 500 Ma (Cambrian). The preliminary chemical data from undated mafic magmatic rocks suggest a supra-subduction zone environment of its formation. The plagioclase-rich nature of paragneisses suggests accumulation of plagioclase, which also argues for volcanosedimentary rocks in a supra-subduction environment with an Early Proterozoic (Late Neoarchean) hinterland. Some preliminary major and trace elements reported by Neubauer et al. (1992) indicate a

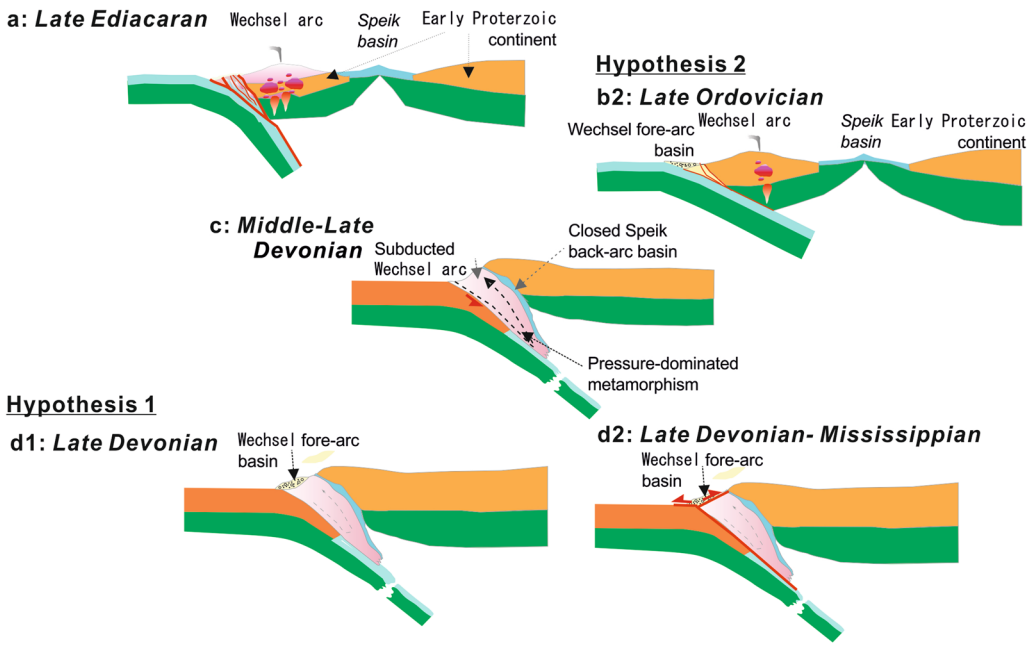

Fig. 17 Tectonic model for the Wechsel basement. For discussion and explanation of the two alternative scenarios, see text

derivation of the albite-porphyroblast paragneiss from greywackes and shales on geochemical grounds. Concentrating on the dominant 550–570 Ma age population argues for a late Ediacaran magmatic arc-related environment (Fig. 17a). The impregnation with graphite, the occurrence of black micaschist and black quartzite indicate a partly anoxic depositional environment. The white, pure quartzite with rounded zircons also indicates input of mature, recycled quartz-arenites, which can only envisaged with continental crust as a hinterland. Altogether, including the prominent Neoarchean to Early Proterozoic and Late Ediacaran-Cambrian sources, an active continental margin can be envisaged as the area of deposition.

Interestingly, the Speik Complex of the Austroalpine basement in the Eastern Alps (see Fig. 1a for location) is an ophiolite that formed in a supra-subduction zone environment at ca. 550 Ma (Melcher and Meisel 2004), which is close to the prominent 550–570 Ma detrital zircon age-group in the Variegated Wechsel Gneiss Complex. We, therefore propose a subduction environment, where a major ocean, potentially Prototethys with either (1) the ophiolitic Speik complex as part of the subducting Prototethys Ocean or (2) the Speik Complex formed as a back-arc basin behind a magmatic arc that separated the Wechsel arc from an early Proterozoic continental hinterland (Fig. 17a).

For the further tectonic evolution, we distinguish, according to the age uncertainty of the Wechsel Phyllite Unit, between Hypothesis 1 with a Late Devonian (to potentially Mississippian) age and Hypothesis 2 with a Late Ordovician age. In Hypothesis 1, during the next step, during Middle to early Late Devonian times, the back-arc basin closed, and a part of the back arc basin subducted together with the Wechsel arc, which was affected by pressure-dominated metamorphism during this time (Fig. 17c). In Hypothesis 2, the protoliths of the Wechsel Phyllite Unit were deposited in a fore-arc setting during Late Ordovician recycling material from the Wechsel arc (Fig. 17b2) followed by metamorphic overprint of the Wechsel arc (Fig. 17c). Finally, the deformed and metamorphosed Wechsel arc was exhumed and a basin formed in front of the exhuming arc and, in Hypothesis 1, recycled Wechsel arc material was deposited in a short-living Wechsel fore-arc-type basin (Fig. 17d1), whereas in Hypothesis 2, the Wechsel Phyllite Unit is tectonically emplaced over the Monotonous and Variegated Wechsel Gneiss Complex (Fig. 17d2).

6.4 The Wechsel basement within the Austroalpine basement

Late Neoproterozoic to Cambrian detritus and arc-related units are common in the central European Variscides (e.g., Neubauer 2002; von Raumer et al. 2013; Stephan et al. 2019 and references therein) and within the Austroalpine nappe complex of the Eastern (Handler et al. 1997; Neubauer 2002, 2014; Haas et al. 2020) and Southern Alps (Dallmeyer and Neubauer 1994; Arboit

et al. 2018). The age populations of 520 and 550–570 Ma are rather unique for the Wechsel basement. Detrital zircon ages of 559 to 572 Ma were found in paragneisses of Seckau basement (Mandl et al. 2018; Fig. 1a). Ages at ca. 500 Ma of acidic magmatic rocks are known from metaconglomerates covering amphibolite-grade basement (Kaintaleck slices) of the Eastern Greywacke zone (Fig. 1a) (Neubauer et al. 2002) and from the S-type Hochreichart Plutonic Suite in the Seckau basement (Mandl et al. 2018; Fig. 1a). In the Silvretta basement, oceanic plagiogranite with an age of 532 ± 30 Ma (Müller et al. 1996) occurs together with the calc-alkaline older orthogneisses with U–Pb zircon ages of 519–568 Ma (Müller et al. 1995; Schaltegger et al. 1997). Furthermore, calcalkaline amphibolites with an age of 529 +9/−8 Ma are associated with these orthgneisses in the western Silvretta basement (Nilius et al. 2016). Consequently, although the macroscopic appearance is not similar, Cambrian magmatic arc and potential oceanic elements are known from several elements in the Austroalpine nappe stack as in the Wechsel magmatic arc together with Late Ediacaran detrital detritus. An interesting common feature is the occurrence of leucocratic granitic gneisses with an age of ca. 500 Ma in the Variegated Wechsel Gneiss Complex, Seckau basement and as boulders on the Kaintaleck basement.

There is a general consensus that all these Alpine units mentioned above and the basement units of central European Variscides did split off from northern Gondwana. Similar arc systems are common in northeast African-Arabian sector (von Raumer et al. 2013; Haas et al. 2020). However, another critical element is the evidence for abundant 2.1 to 2.2 Ga and 2.5 to 2.8 Ga age signatures in metasedimentary rocks, which call for an Upper Neoarchean and Lower Proterozoic continental crust as a nearby source. Such tectonic elements are characteristic for both West and Northeast Africa and Amazonia (Stephan et al. 2019). The model proposed here (Fig. 18) is based on the recent proposal of Haas et al. (2020) but with the major difference that a West African palaeogeographic relationship for Cambrian time is preferred because of the following reasons. Northwest Africa is characterized by two zircon age populations: Late Archean and Early Proterozoic (Eburnean: ca. 2.1 Ga), and both age populations are prominent in the Wechsel basement. Furthermore, Late Ediacaran/Cambrian arc systems extend to South America (e.g., Ribeiro belt; Heilbron et al. 2020). Consequently, we adopt the Northwest African relationship in Fig. 18, although we cannot fully exclude the "out of NE-Africa" hypothesis of Haas et al. (2020). The new data shows the close relationship of the Wechsel arc to northwestern Gondwana prominent in both West and Northeast Africa and Amazonia (Stephan et al. (2019).

Finally, we also note that the U–Pb zircon age populations of both the Variegated Wechsel Gneiss Complex and the Wechsel Phyllite Unit are largely dissimilar to equivalent Pennsylvanian to Lower Triassic sandstones from higher tectonic units of the Austroalpine nappe stack as recently proposed by Haas et al. (2020). Consequently, we propose that the Wechsel basement has a unique origin and differs in the history from the higher

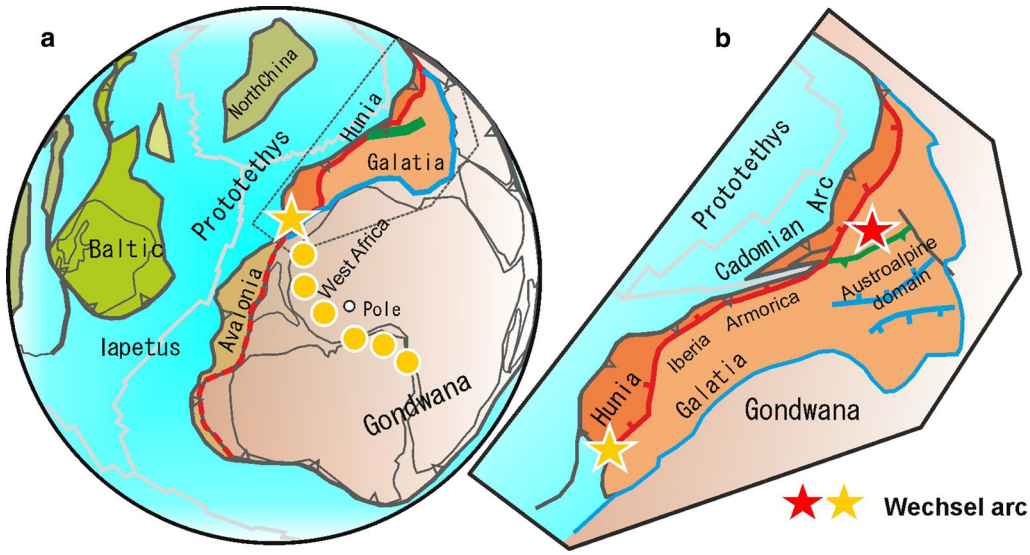

Fig. 18 Potential palaeogeographic relationships. The model for the suggested position of Wechsel arc is based on the recent proposal of Haas et al. (2020) (red star) with the major difference that a West African palaeogeographic relationship for the Cambrian is preferred (yellow star) (see text for discussion). Circles indicate the Late Archean/Early Proterozoic (Eburnean) crust and Late Ediacaran/Cambrian arc systems, which extend to South America (e.g., Ribeiro belt)

Austroalpine basement units although the Late Ediacaran and Cambrian detrital zircon age components were found both in the Silvretta and Seckau basement.

7 Conclusions

The new age data from the Variegated Wechsel Gneiss complex give evidence for several stages of continental arc-like magmatism, predominantly at 550–570 Ma, and subordinately at 530 Ma and 500 Ma. We speculate on a potential relationships of the continental arc-type magmatism at 550–570 Ma and potential oceanic lithosphere (Speik complex) of Proto-Tethyan affinity, which is also preserved in the Austroalpine nappe complex (Neubauer 2002 and references therein). We argue, therefore, for a long-lasting Late Neoproterozoic to Cambrian subduction of potentially Proto-Tethyan origin along the northwestern margins of Gondwana although a northeastern Africa-Arabian origin cannot fully excluded. The abundant, nearly 2.1 to 2.2 Ga- and 2.5 to 2.8 Ga age signatures call for a Neoarchean and Lower Proterozoic continental crust in the nearby source showing the close relationship to northern Gondwana prominent in both West and Northeast Africa and Amazonia (Stephan et al. (2019).

The Wechsel Phyllite Unit overlying the Monotonous Wechsel Gneiss Complex has been deposited not earlier than Late Ordovician and is likely postdating Middle to early Late Devonian pressure-dominated metamorphism of the Monotonous and Variegated Wechsel Gneiss Complexes. The Wechsel Phyllite Unit contains mainly detritus derived from the Variegated Wechsel Gneiss Complex in the footwall.

Supplementary information

Supplementary information accompanies this paper at https://doi.org/10.1186/s00015-020-00373-3.

Additional file 1: Figure S1. Representative thin section photomicrographs of studied rocks of the Variegated Wechsel Gneiss Complex. All are with crossed polarizers. The scale bar at lower right represents 500 µm. Abbreviations: Amp: amphibole, Chl: chlorite, Czo: clinozoisite, Grt: garnet, Kf: K-feldspar, Pl: plagioclase, Opq: opaque mineral, Qz: quartz, Pl-PB: albite porphyroblast, Ser: sericite, WM: white mica.

Additional file 2: Figure S2. Representative thin section photomicrographs of studied rocks (metatuffites) of the Wechsel Phyllite Unit. (a) Long axis is 5.5 cm. (b) Long axis is 1.4 cm. Abbreviations: Chl: chlorite, GM: graphitic material, Kf: K-feldspar, Pl: plagioclase, Qz: quartz, Ser: sericite, S1, S2: foliation S_1 and foliation S_2.

Additional file 3: Table S1. Analytical U–Pb zircon dating results from the Variegated Wechsel Gneiss Complex.

Additional file 4: Table S2. Analytical U–Pb zircon dating results from the Wechsel Phyllite Unit.

Acknowledgements
We gratefully acknowledge critical comments and suggestions by Christoph Hauzenberger, an anonymous reviewer and by the guest editor Otmar Müntener to the initial version of manuscript. These helped to clarify science and readability of the paper.

Authors' contributions
FN and Y-JL designed the study and collected the samples together with SY, JG, RC, S-YY and BL Analytical work was mostly done by S-YY, Q-BG. All authors contributed to the interpretation of data, preparation of figures and writing of the paper under the lead of FN. All authors read and approved the final manuscript.

Funding
We acknowledge funding from the NFSC (Nos. 91755212; 41772200) together with the Qingdao Leading innovation talents (19-3-2-19-zhc) to Y. Liu.

Availability of data and materials
The entire new data set is included in the paper.

Ethics approval and consent to participate
Not applicable.

Consent for publication
Not applicable.

Competing interests
The authors declare that they have no competing interests.

Author details
[1] Department of Geography and Geology, Geology Division, Paris-Lodron-University of Salzburg, Hellbrunnerstraße 34, 5020 Salzburg, Austria. [2] Key Lab of Submarine Geoscience and Prospecting Techniques, MOE, Institute for Advanced Ocean Study, College of Marine Geosciences, Ocean University of China, Qingdao 266100, China. [3] Ocean University of China, Qingdao 266100, China. [4] College of Earth Science, Institute of Disaster Prevention, Sanhe 065201, Hebei, China.

Received: 18 April 2020 Accepted: 19 October 2020
Published online: 25 November 2020

References

Andersen, T. (2002). Correction of common lead in U-Pb analyses that do not report ^{204}Pb. *Chemical Geology, 192,* 59–79. https://doi.org/10.1016/S0009-2541(02)00195-X.

Angeiras, A. G. (1967). Geology of Kirchberg am Wechsel and Molz Valley Areas (Semmering Window), Lower Austria. *Jahrbuch der Geologischen Bundesanstalt, 110,* 217–243.

Arboit, F., Chew, D., Visoná, D., Massironi, M., Sciascia, F., Benedetti, G., et al. (2018). The geodynamic evolution of the Italian South Alpine basement from the Ediacaran to the Carboniferous: was the South Alpine terrane part of the peri-Gondwana arc-forming terranes? *Gondwana Research, 65,* 17–30.

Boynton, W. V. (1984). Geochemistry of the rare earth elements: meteorite studies. In P. Henderson (Ed.), *Rare Earth Element Geochemistry* (pp. 63–114). Amsterdam: Elsevier.

Cohen, K. M., Finney, S. C., Gibbard, P. L., & Fan, J.-X. (2013). The ICS International Chronostratigraphic Chart. *Episodes, 36,* 199–204.

Corfu, F., Hanchar, J. M., Hoskin, P. W. O., & Kinny, P. (2003). Atlas of zircon textures. *Reviews in Mineralogy and Geochemistry, 53,* 469–500. https://doi.org/10.2113/0530469.

Dallmeyer, R. D., & Neubauer, F. (1994). ^{40}Ar/^{39}Ar age of detrital muscovites, Carnic Alps: evidence for a Cadomian linkage in the Eastern Alps. *Journal of the Geological Society [London], 151,* 591–598.

Dallmeyer, R. D., Neubauer, F., Handler, R., Fritz, H., Müller, W., Pana, D., et al. (1996). Tectonothermal evolution of the internal Alps and Carpathians: ^{40}Ar/^{39}Ar mineral and whole rock data. *Eclogae Geologicae Helvetiae, 89,* 203–227.

Faupl, P. (1970a). Zur Geologie des NW-Abschnitts des Wechselgebietes zwischen Trattenbach (NÖ) und Fröschnitz (Stmk.) — Österreich. *Mitteilungen der Gesellschaft der Geologie- und Bergbaustudenten (Wien), 19,* 27–70.

Faupl, P. (1970b). Zur Geologie und Petrographie des südlichen Wechselgebietes. *Mitteilungen der Geologischen Gesellschaft in Wien, 63,* 22–51.

Flajs, M., & Schönlaub, H. P. (1976). Die biostratigraphische Gliederung des Altpaläozoikums am Polster bei Eisenerz (Nördliche Grauwackenzone, Österreich). *Verhandlungen der. Geologischen Bundesanstalt (Wien), 1976,* 257–303.

Haas, I., Eichinger, S., Haller, D., Fritz, H., Nievoll, J., Mandl, M., et al. (2020). Gondwana fragments in the Eastern Alps: A travel story from U/Pb zircon data. *Gondwana Research, 77,* 204–222.

Handler, R., Dallmeyer, R. D., & Neubauer, F. (1997). $^{40}Ar/^{39}Ar$ ages of detrital white micas from Upper Austroalpine units in the Eastern Alps, Austria: Evidence for Cadomian and contrasting Variscan sources. *Geologische Rundschau, 86,* 69–80.

Harley, S. L., Kelly, N. M., & Möller, A. (2007). Zircon behaviour and the thermal histories of mountain chains. *Elements, 3,* 25–30.

Heilbron, M., Morisson Valeriano, C., Tupinambá, M., Peixoto, C., Neubauer, F., Dussin, I., et al. (2020). Neoproterozoic magmatic arc systems of the central Ribeira belt, SE-Brazil, in the context of West-Gondwana pre-collisional history: a review. *Journal of South American Earth Sciences*, *103*, 102710. https://doi.org/10.1016/j.jsames.2020.102710.

Heinrichs, T., Siegesmund, S., Frei, D., Drobe, M., & Schulz, B. (2012). Provenance signatures from whole-rock geochemistry and detrital zircon ages of metasediments from the Austroalpine basement south of the Tauern Window. *Geo Alp, 9,* 156–185.

Herrmann, P., Mandl, G.W., Matura, A., Neubauer, F., Riedmüller, G. & Tollmann, A. (1991). Geologische Karte der Republik Österreich 1 : 50.000; 105 Neunkirchen. Wien: Geologische Bundesanstalt.

Hoinkes, G., Koller, F., Rantitsch, G., Dachs, E., Hock, V., Neubauer, F., et al. (1999). Alpine metamorphism of the Eastern Alps. *Schweizerische Mineralogische und Petrographische Mitteilungen, 79,* 155–181.

Hoskin, P. W. O., & Schaltegger, U. (2003). The composition of zircon and igneous and metamorphic petrogenesis. *Reviews in Mineralogy and Geochemistry, 53,* 27–62. https://doi.org/10.2113/0530027.

Hou, K. J., Li, Y. H., & Tian, Y. Y. (2009). In situ U-Pb zircon dating using laser ablation-multi ion counting-ICP-MS. *Mineral Deposits, 28*(4), 481–492. **(In Chinese with English abstract)**.

Huska, G. (1970). Zur Geologie der Umgebung von Waldbach, südwestliches Wechselgebiet, Steiermark. *Verhandlungen der Geologischen Bundesanstalt, 1970,* 61–65.

Huska, G. (1971). Zur Geologie und Tektonik der Weißerdelagerstätte Aspang am Ostrand des Wechselfensters (Niederösterreich). *Mitteilungen der Geologischen Gesellschaft in Wien, 64,* 109–136.

Jochum, K. P., Willbold, M., Raczek, I., Stoll, B., & Herwig, K. (2005). Chemical Characterisation of the USGS Reference Glasses GSA-1G, GSC-1G, GSD-1G, GSE-1G, BCR-2G, BHVO-2G and BIR-1G Using EPMA, ID-TIMS, ID-ICP-MS and LA-ICP-MS. *Geostandards and Geoanalytical Research, 29*(3), 285–302.

Kreuss, O. (2015). *GEOFAST 50 000 136 Hartberg*. Wien: Geologische Bundesanstalt.

Liu, Y. S., Gao, S., Hu, Z. C., Gao, C. G., Zong, K. Q., & Wang, D. B. (2010). Continental and oceanic crust recycling-induced melt–peridotite interactions in the Trans-North China Orogen: U-Pb dating, Hf isotopes and trace elements in zircons from mantle xenoliths. *Journal of Petrology, 51,* 537–571.

Loeschke, J., & Heinisch, H. (1993). Palaeozoic volcanism in the Eastern Alps and its Palaeotectonic significance. In J. von Raumer & F. Neubauer (Eds.), *Pre-Mesozoic Geology in the Alps* (pp. 441–455). Berlin: Springer.

Ludwig, K. R. (2012), User's Manual for Isoplot3.75 – A Geochronological Toolkit for Microsoft Excel. Berkeley, Geochronological Center Special Publication, No. 5.

Mandl, M., Kurz, W., Hauzenberger, C., Fritz, H., Klötzli, U., & Schuster, R. (2018). Pre-Alpine evolution of the Seckau Complex (Austroalpine basement/Eastern Alps): Constraints from in situ LA-ICP-MS U-Pb zircon geochronology. *Lithos, 296–299,* 412–430.

Melcher, F., & Meisel, T. (2004). A Metamorphosed Early Cambrian Crust-Mantle Transition in the Eastern Alps, Austria. *Journal of Petrology, 45,* 1689–1723. https://doi.org/10.1093/petrology/egh030.

Meli, S., & Klötzli, U. S. (2001). Evidence for Lower Paleozoic magmatism in the Eastern Southalpine basement: zircon geochronology from Comelico porphyroids. *Schweizerische Mineralogische und Petrographische Mitteilungen, 81,* 147–157.

Mohr, H. (1912). Versuch einer tektonischen Auflösung des Nordostsporns der Zentralalpen. *Denkschriften der k. & k. Akademie der Wissenschaften, mathematisch-naturwissenschaftliche Klasse, 88,* 633–652.

Mohr, H. (1913). Geologie der Wechselbahn (insbes. des Großen Hartbergtunnels). *Denkschriften der k. & k. Akademie der Wissenschaften, mathematisch-naturwissenschaftliche Klasse, 87,* 321–379.

Müller, W., Dallmeyer, R. D., Neubauer, F., & Thöni, M. (1999). Deformation-induced resetting of Rb/Sr and $^{40}Ar/^{39}Ar$ mineral systems in a low-grade, polymetamorphic terrane (eastern Alps, Austria). *Journal of the Geological Society (London), 156,* 261–278.

Müller, B., Klötzli, U., & Flisch, M. (1995). U-Pb and Pb-Pb zircon dating of the older orthogneiss suite in the Silvretta nappe, eastern Alps: Cadomian magmatism in the upper Austro-Alpine realm. *Geologische Rundschau, 84,* 457–465.

Müller, B., Klötzli, U. S., Schaltegger, U., & Flisch, M. (1996). Early Cambrian oceanic plagiogranite in the Silvretta Nappe, eastern Alps: geochemical, zircon U-Pb and Rb-Sr data from garnethornblende-plagioclase gneisses. *Geologische Rundschau, 85,* 822–831.

Neubauer, F. R. (1983). Bericht 1979 über geologische Aufnahmen im Kristallin auf den Blättern 105 Neunkirchen und 136 Hartberg. *Verhandlungen der. Geologischen Bundesanstalt (Wien), 1980*(1), A75–A79.

Neubauer, F. (1994). Comment to M. Wagreich, Subcrustal tectonic erosion in orogenic belts A model for the Late Cretaceous subsidence of the Northern Calcareous Alps (Austria). *Geology, 22,* 855–856.

Neubauer, F. (2002). Evolution of late Neoproterozoic to early Paleozoic tectonic elements in central and southeast European Alpine mountain belts: review and synthesis. *Tectonophysics, 352,* 87–103.

Neubauer, F. (2014). Gondwana-Land goes Europe. *Austrian Journal of Earth Sciences, 107*(1), 147–155.

Neubauer, F., & Frisch, W. (1993). The Austroalpine metamorphic basement east of the Tauern window. In J. von Raumer & F. Neubauer (Eds.), *Pre-Mesozoic Geology in the Alps* (pp. 515–536). Berlin: Springer.

Neubauer, F., Frisch, W., & Hansen, B. T. (2002). Early Palaeozoic tectonothermal events in basement complexes of the eastern Graywacke Zone (Eastern Alps. evidence from U-Pb zircon data. *International Journal of Earth Sciences, 91,* 775–786.

Neubauer, F., Frisch, W., Schmerold, R., & Schlöser, H. (1989). Metamorphosed and dismembered ophiolite suites in the basement units of the Eastern Alps. *Tectonophysics, 164,* 49–62.

Neubauer, F., Hoinkes, G., Sassi, F. P., Handler, R., Höck, V., Koller, F., et al. (1999). Pre-Alpine metamorphism of the Eastern Alps. *Schweizerische Mineralogische und Petrographische Mitteilungen, 79,* 41–62.

Neubauer, F., Müller, W., Peindl, P., Moyschewitz, G., Wallbrecher, E., & Thöni, M. (1992). Evolution of Lower Austroalpine units along the eastern margins of the Alps. In F. Neubauer (Ed.), *ALCAPA Field Guide—The Eastern Central Alps of Austria* (pp. 97–114). Austria: University of Graz.

Neubauer, F., & Sassi, F. P. (1993). The quartzphyllite and related units of the Austro-Alpine domain. In J. von Raumer & F. Neubauer (Eds.), *Pre-Mesozoic Geology in the Alps* (pp. 423–439). Berlin: Springer.

Nilius, N.-P., Froitzheim, N., Nagel, T. J., Tomascheck, F., & Heuser, A. (2016). The Schwarzhorn Amphibolite (Eastern Rätikon, Austria): an Early Cambrian intrusion in the Lower Austroalpine basement. *Geologica Carpathica, 67*(2), 121–132.

Pearce, J. A., & Cann, J. R. (1973). Tectonic setting of basic volcanic rocks determined using trace element analyses. *Earth and Planetary Science Letters, 19,* 290–300.

Putiš, M., Ivan, P., Kohút, M., Spišiak, J., Siman, P., Radvanec, M., et al. (2009). Meta-igneous rocks of the Western Carpathian basement: indicator of Early Paleozoic extension and shortening events. *Bulletin de Societé Géologique de France, 180,* 461–471.

Richarz, P. S. (1911). Die Umgebung von Aspang am Wechsel (NÖ). *Jahrbuch der k. & k. Geologischen Reichsanstalt: (Wien), 61*(2), 285–338.

Schaltegger, U., Nägler, T. F., Corfu, F., Maggetti, M., Galetti, G., & Stosch, H. G. (1997). A Cambrian island arc in the Silvretta nappe: constraints from geochemistry and geochronology. *Schweizerische Mineralogische und Petrographische Mitteilungen, 77,* 337–350.

Schönlaub, H. P., & Heinisch, H. (1993). The Classic Fossiliferous Palaeozoic Units of the Eastern and Southern Alps. In J. F. von Raumer & F. Neubauer (Eds.), *Pre-Mesozoic Geology in the Alps* (pp. 395–422). Heidelberg: Springer.

Schulz, B., Bombach, K., Pawlig, S., & Brätz, H. (2004). Neoproterozoic to early-Palaeozoic magmatic evolution in the Gondwana-derived Austroalpine basement to the south of the Tauern Window (Eastern Alps). *International Journal of Earth Sciences, 93,* 824–843.
Schulz, B., Steenken, A., & Siegesmund, S. (2008). Geodynamic evolution of an Alpine terrane: the Austroalpine basement to the south of the Tauern Window as a part of the Adriatic Plate (Eastern Alps). *Geological Society, (London) Special Publication, 298,* 5–44.
Schwinner, R. (1932). Zur Geologie der Oststeiermark: Die Gesteine und ihre Vergesellschaftung. *Sitzungsberichte der Akademie der Wissenschaften Wien, mathematisch-naturwissenschaftliche Klasse, 141,* 319–358.
Shakerardakani, F., Li, X.-H., Neubauer, F., Ling, X.-X., Li, J., Monfaredi, B., et al. (2020). Genesis of Early Cretaceous leucogranites in the central Sanandaj-Sirjan zone, Iran: Reworking of Neoproterozoic metasedimentary rocks in an active continental margin. *Lithos, 352–353,* 105330.
Siegesmund, S., Heinrichs, T., Romer, R. L., & Doman, D. (2007). Age constraints on the evolution of the Austroalpine basement to the south of the Tauern Window. *International Journal of Earth Sciences, 96,* 415–432.
Siegesmund, S., Oriolo, S., Heinrichs, T., Basei, M. A. S., Nolte, N., Hüttenrauch, F., et al. (2018). Provenance of Austroalpine basement metasediments: tightening up Early Palaeozoic connections between peri-Gondwanan domains of central Europe and Northern Africa. *International Journal of Earth Sciences, 107,* 2293–2315. https://doi.org/10.1007/s00531-018-1599-5.
Söllner, F., Miller, H., & Höll, R. (1997). Alter und Genese rhyodazitischer Metavulkanite („Porphyroide") der Nördlichen Grauwackenzone und der Karnischen Alpen (Österreich): Ergebnisse von U-Pb-Zirkondatierungen. *Zeitschrift der Deutschen Geologischen Gesellschaft, 148,* 499–522.
Stephan, T., Kroner, U., & Romer, R. L. (2019). The pre-orogenic detrital zircon record of the Peri-Gondwanan crust. *Geological Magazine, 156*(2), 281–307.
Thöni, M. (1999). A review of geochronological data from the Eastern Alps. *Schweizerische Mineralogische und Petrographische Mitteilungen, 79,* 209–230.
Thöni, M. (2006). Dating eclogite-facies metamorphism in the Eastern Alps – approaches, results, interpretations: a review. *Mineralogy and Petrology, 88,* 123–148. https://doi.org/10.1007/s00710-006-0153-5.
Tollmann, A. (1977). *Geologie von Österreich Band I: Die Zentralalpen* (p. 766). Vienna: Deuticke.
Vetters, W. (1970). Zur Geologie des SW-Abschnittes des Wechselgebietes zwischen Rettenegg —Feistritzwald (Steiermark). *Mitteilungen der Gesellschaft der Geologie- und Bergbaustudenten (Wien), 19,* 71–102.
von Raumer, J., Bussy, F., Schaltegger, U., Schulz, B., & Stampfli, G. M. (2013). Pre-Mesozoic Alpine basements—Their place in the European Paleozoic framework. *Geological Society of America Bulletin, 125,* 14–32.
Vozárová, A., Nickolay Rodionov, N., Šarinová, K., & Presnyakov, S. (2017). New zircon ages on the Cambrian-Ordovician volcanism of the Southern Gemericum basement (Western Carpathians, Slovakia): SHRIMP dating, geochemistry and provenance. *International Journal of Earth Sciences, 106,* 2147–2170.
Vozárová, A., Šarinová, K., Radionov, N., Laurinc, D., Padarin, I., Sergeev, S., et al. (2012). U-Pb ages of detrital zircons from Paleozoic metasandstones of the Gelnica Terrane (Southern Gemeric Unit, Western Carpathians, Slovakia): evidence for Avalonian-Amazonian provenance. *International Journal of Earth Sciences, 101,* 919–936.
Winchester, J. A., & Floyd, P. A. (1977). Geochemical discrimination of different magma series and their differentiation products using immobile elements. *Chemical Geology, 20,* 325–343.
Wood, D. A. (1980). The application of a Th-Hf-Ta diagram to problems of tectonomagmatic classification and to establishing the nature of crustal contamination of basaltic lavas of the British Tertiary Volcanic Province. *Earth and Planetary Science Letters, 50,* 11–30.
Yuan, H. L., Gao, S., Liu, X.-M., Li, H. M., Günther, D., & Wu, F.-Y. (2004). Accurate U-Pb age and trace element determinations of zircon by laser ablation-inductively coupled plasma mass spectrometry. *Geostandards and Geoanalytical Research, 28,* 353–370. https://doi.org/10.1111/j.1751-908X.2004.tb00755.x.
Yuan, S.-H., Neubauer, F., Liu, Y.-J., Genser, J., Liu, B., Yu, S.-Y., et al. (2020). Widespread Permian granite magmatism in Lower Austroalpine units: Significance for Permian rifting in the Eastern Alps. *Swiss Journal of Geosciences*. https://doi.org/10.1186/s00015-020-00371-5.

Publisher's Note